



01 Jan 2002

## Graphite Platelet Nanostructures

Marian Mazurkiewicz

*Missouri University of Science and Technology*

Follow this and additional works at: [https://scholarsmine.mst.edu/min\\_nuceng\\_facwork](https://scholarsmine.mst.edu/min_nuceng_facwork)



Part of the [Mining Engineering Commons](#)

---

### Recommended Citation

M. Mazurkiewicz, "Graphite Platelet Nanostructures," *U.S. Patents*, Jan 2002.

This Patent is brought to you for free and open access by Scholars' Mine. It has been accepted for inclusion in Mining Engineering Faculty Research & Creative Works by an authorized administrator of Scholars' Mine. This work is protected by U. S. Copyright Law. Unauthorized use including reproduction for redistribution requires the permission of the copyright holder. For more information, please contact [scholarsmine@mst.edu](mailto:scholarsmine@mst.edu).



(19) **United States**

(12) **Patent Application Publication**

Mazurkiewicz

(10) **Pub. No.: US 2002/0054995 A1**

(43) **Pub. Date: May 9, 2002**

(54) **GRAPHITE PLATELET NANOSTRUCTURES**

**Publication Classification**

(76) Inventor: **Marian Mazurkiewicz**, Wilkes Barre, PA (US)

(51) **Int. Cl.<sup>7</sup>** ..... **D02G 3/00**  
(52) **U.S. Cl.** ..... **428/364; 241/5; 428/367**

Correspondence Address:

**STERNE, KESSLER, GOLDSTEIN & FOX PLLC**  
**1100 NEW YORK AVENUE, N.W., SUITE 600**  
**WASHINGTON, DC 20005-3934 (US)**

(21) Appl. No.: **09/951,532**

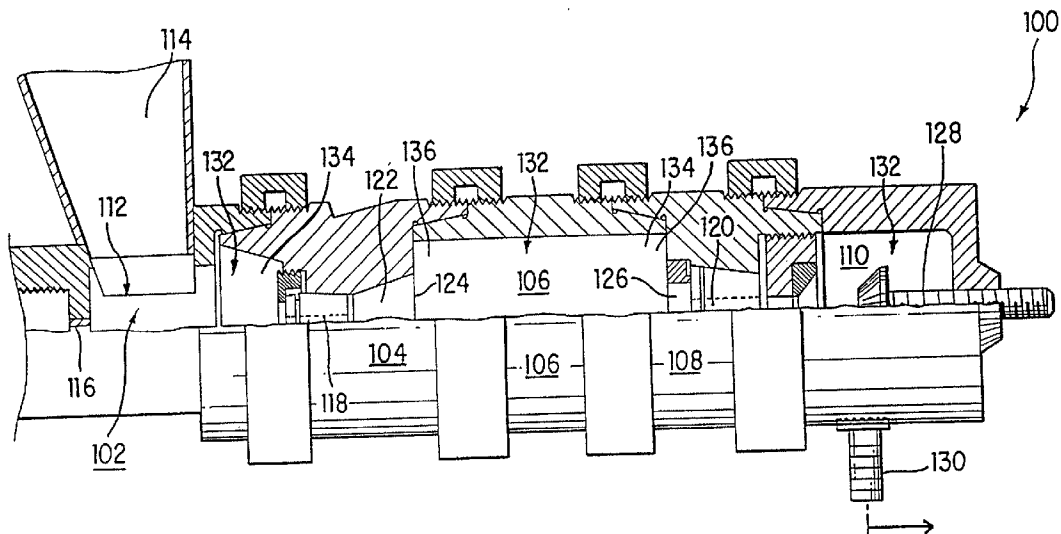
(22) Filed: **Sep. 14, 2001**

**Related U.S. Application Data**

(63) Continuation-in-part of application No. 09/680,273, filed on Oct. 6, 2000, which is a continuation-in-part of application No. 09/413,489, filed on Oct. 6, 1999, now Pat. No. 6,318,649. Continuation-in-part of application No. 09/680,270, filed on Oct. 6, 2000, which is a continuation-in-part of application No. 09/413,489, filed on Oct. 6, 1999, now Pat. No. 6,318,649. Continuation-in-part of application No. 09/680,274, filed on Oct. 6, 2000, which is a continuation-in-part of application No. 09/413,489, filed on Oct. 6, 1999, now Pat. No. 6,318,649. Continuation-in-part of application No. 09/680,271, filed on Oct. 6, 2000, which is a continuation-in-part of application No. 09/413,489, filed on Oct. 6, 1999, now Pat. No. 6,318,649.

(57) **ABSTRACT**

Separated graphite nanostructures are formed of thin graphite platelets having an aspect ratio of at least 1,500:1. The platelets have an angular geometric structure and may be fully independent from an original graphite particle, or partially attached to the particle. The graphite platelets have an average thickness in the range of 1-100 nm. The graphite nanostructures are created from synthetic or natural graphite using a high-pressure mill. Fluid jets of the high-pressure flaking mill cause fluid to enter the tip of cracks in the graphite particles, which creates tension at the tip. This tension causes the cracks to propagate along the natural planes in the graphite so that small particles of the graphite separate into platelets. The platelets can be treated after the milling process by drying the platelets in a spray dryer. The platelets may optionally be introduced into a hydrocyclone to separate the platelets by size. The resulting graphite nanostructures can be added to conventional polymers to create polymer composites having increased mechanical characteristics, including an increased flexural modulus, heat deflection temperature, tensile strength, electrical conductivity, and notched impact strength.



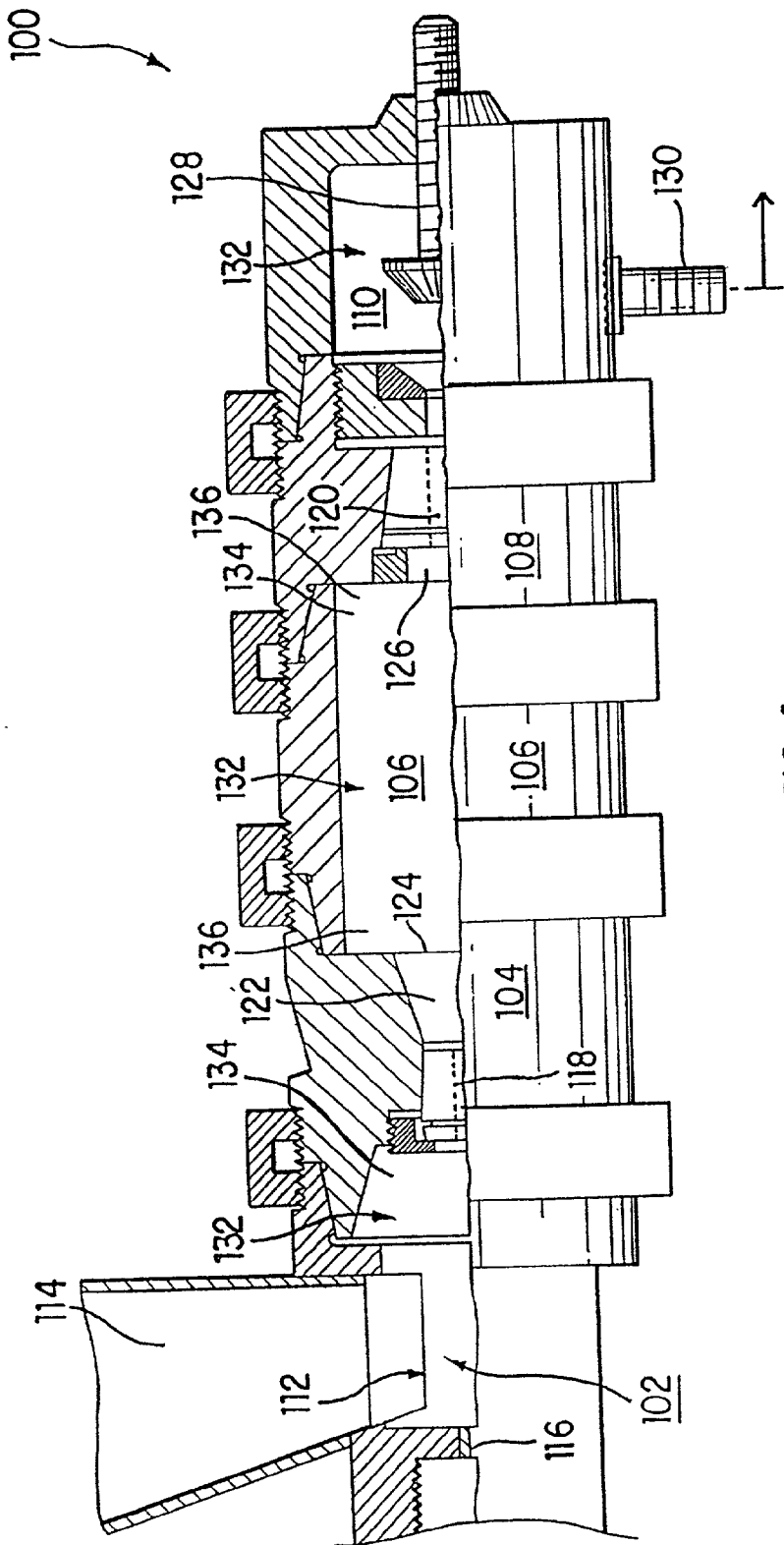


FIG. 1

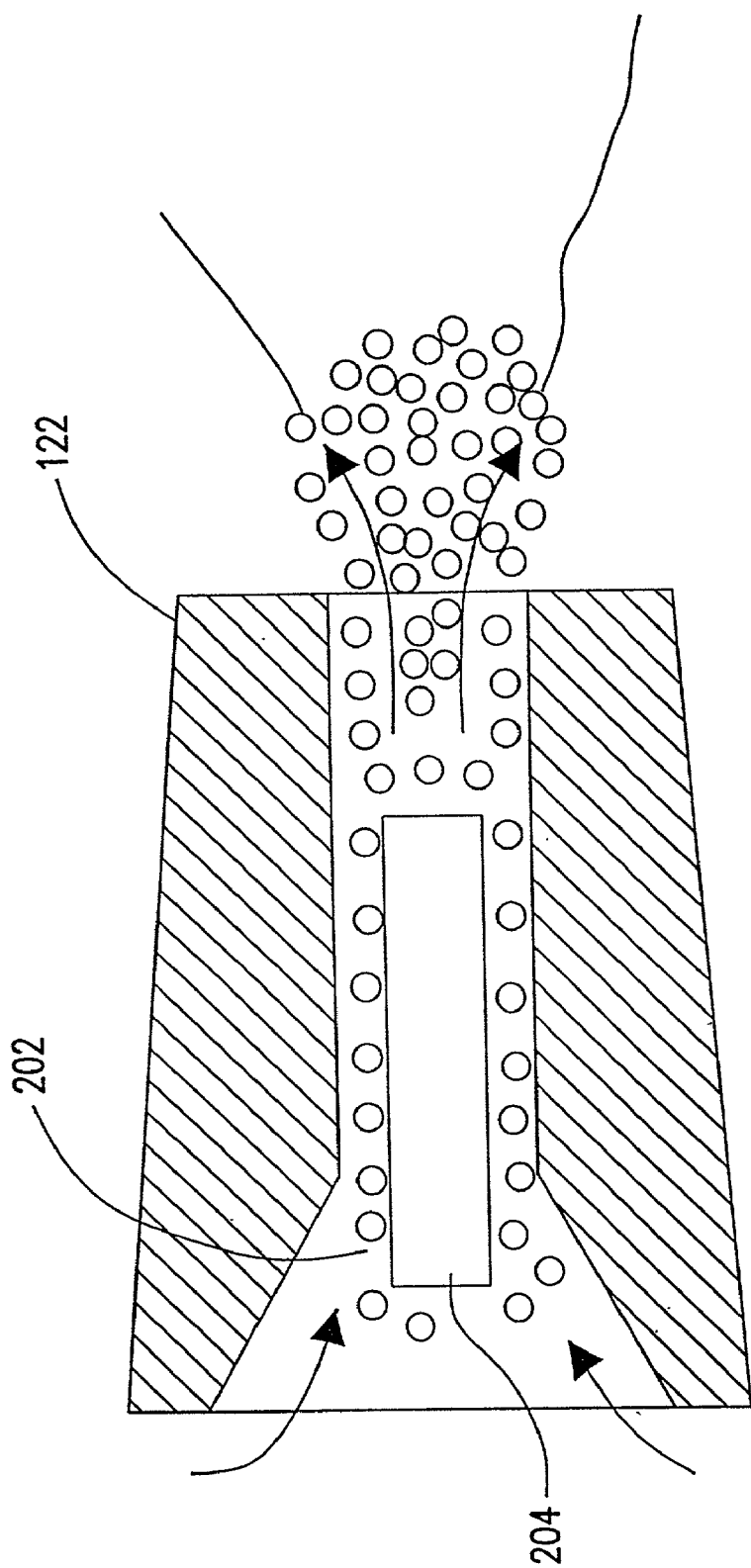


FIG. 2

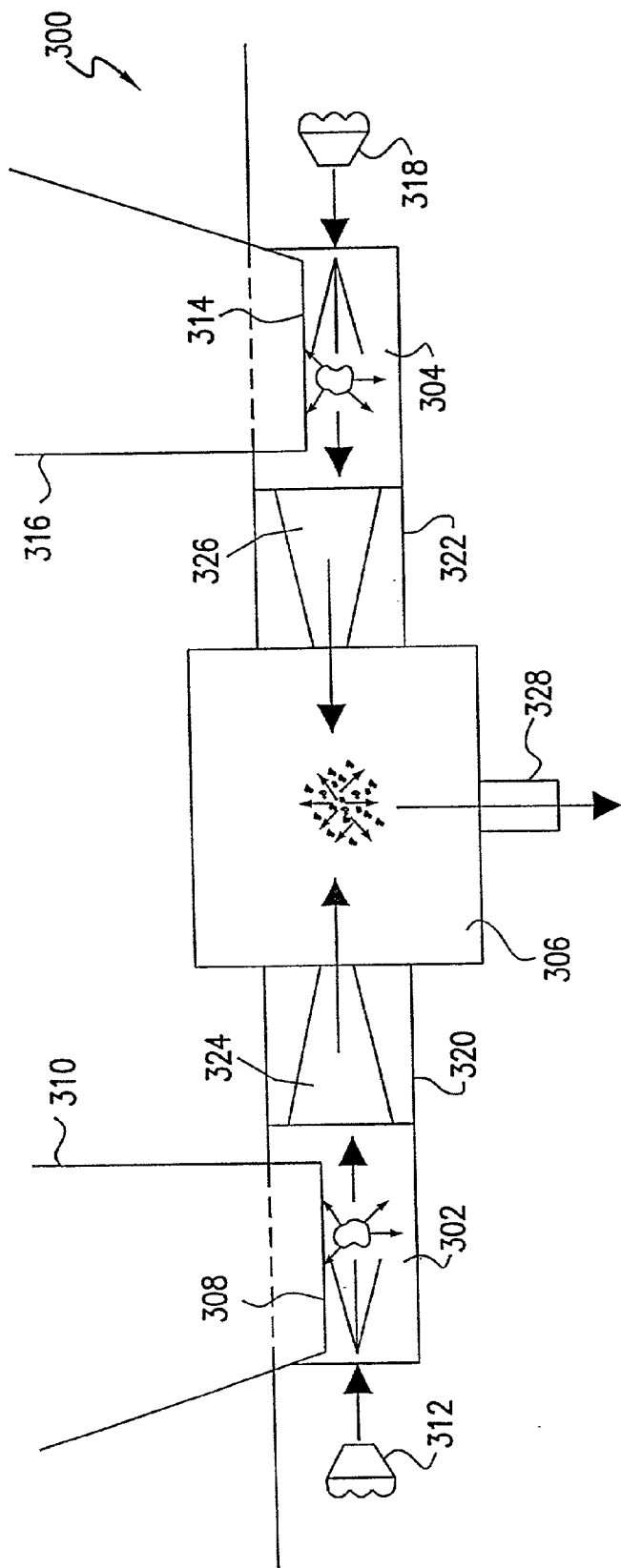


FIG. 3

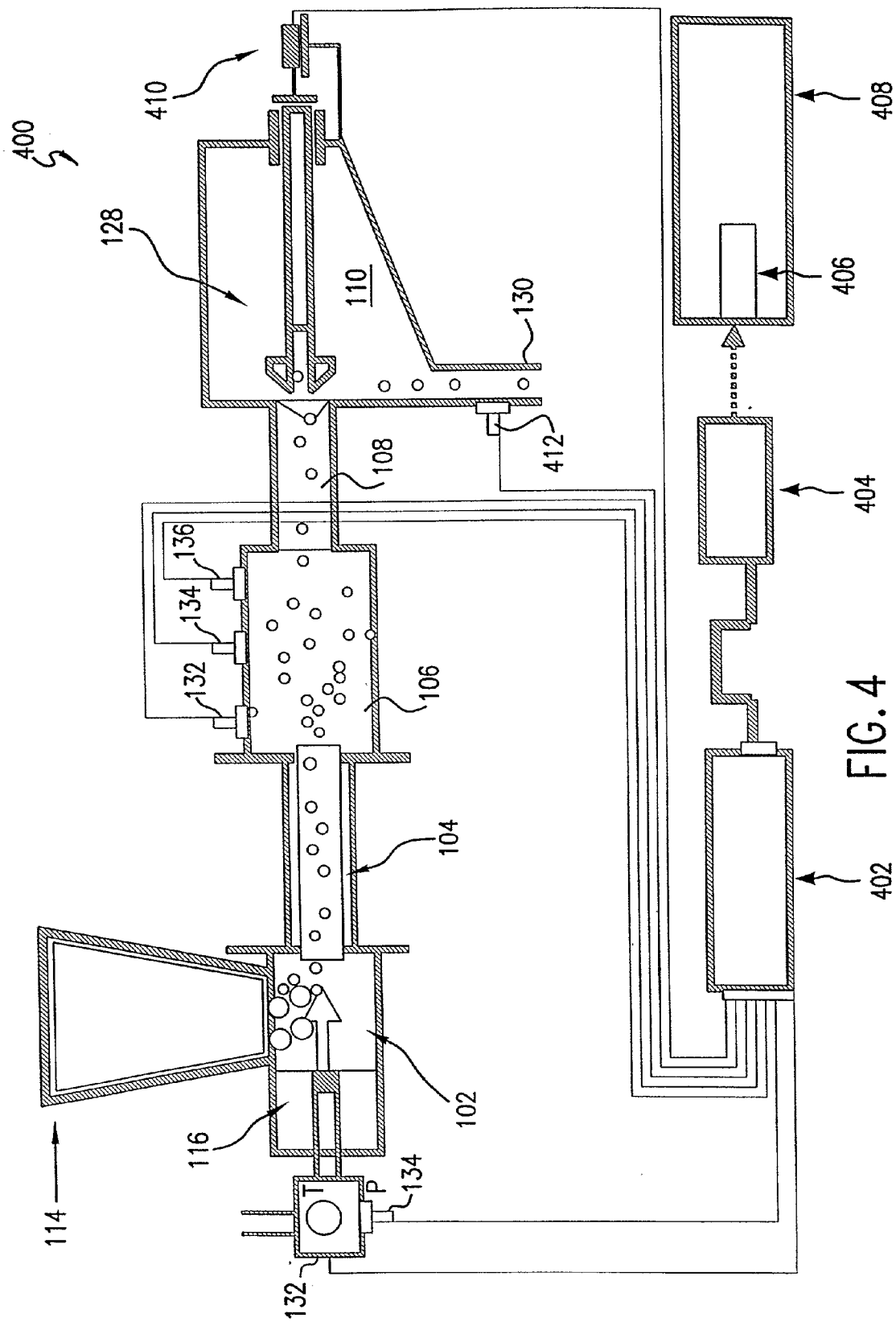


FIG. 4

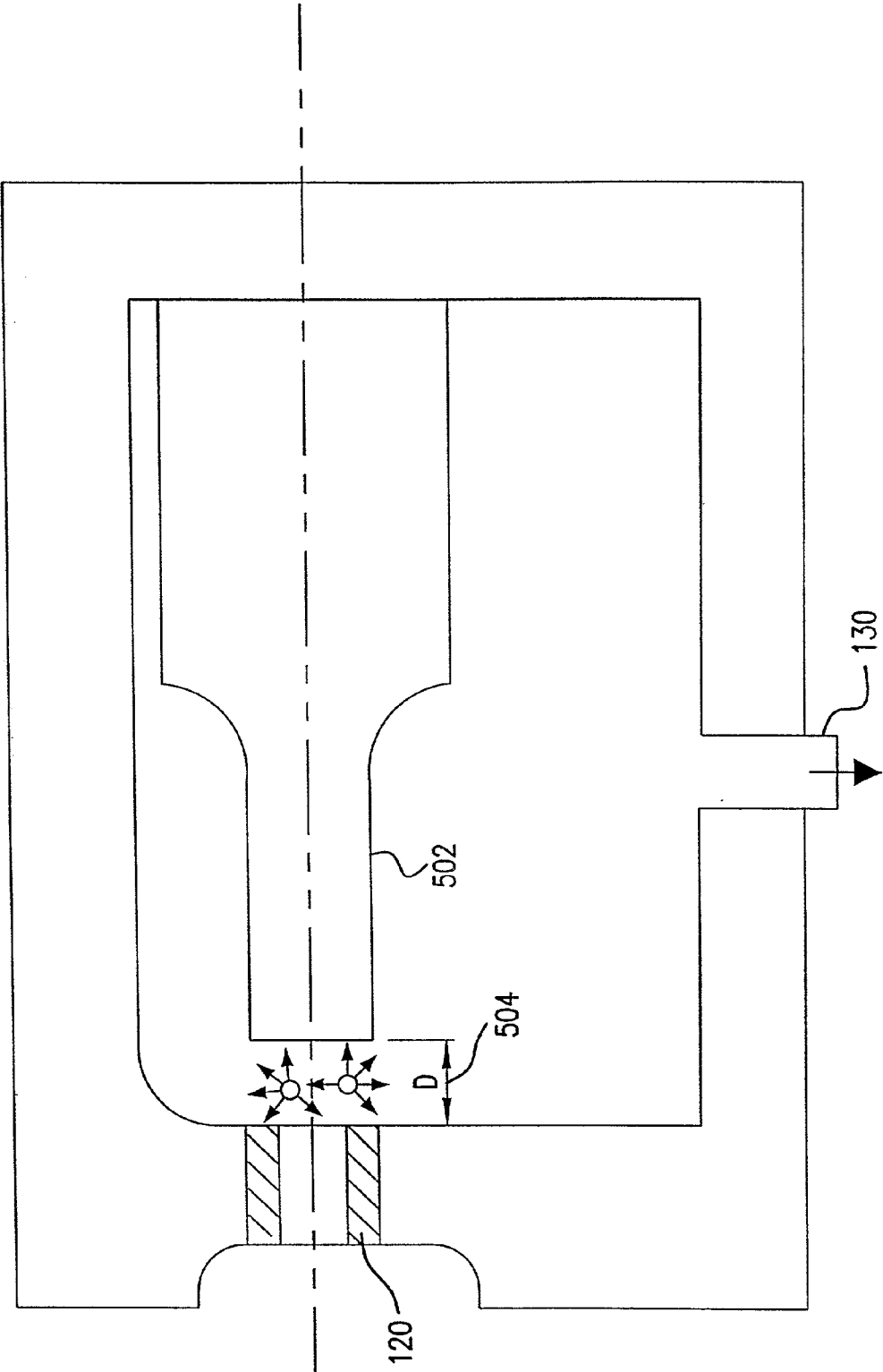


FIG. 5

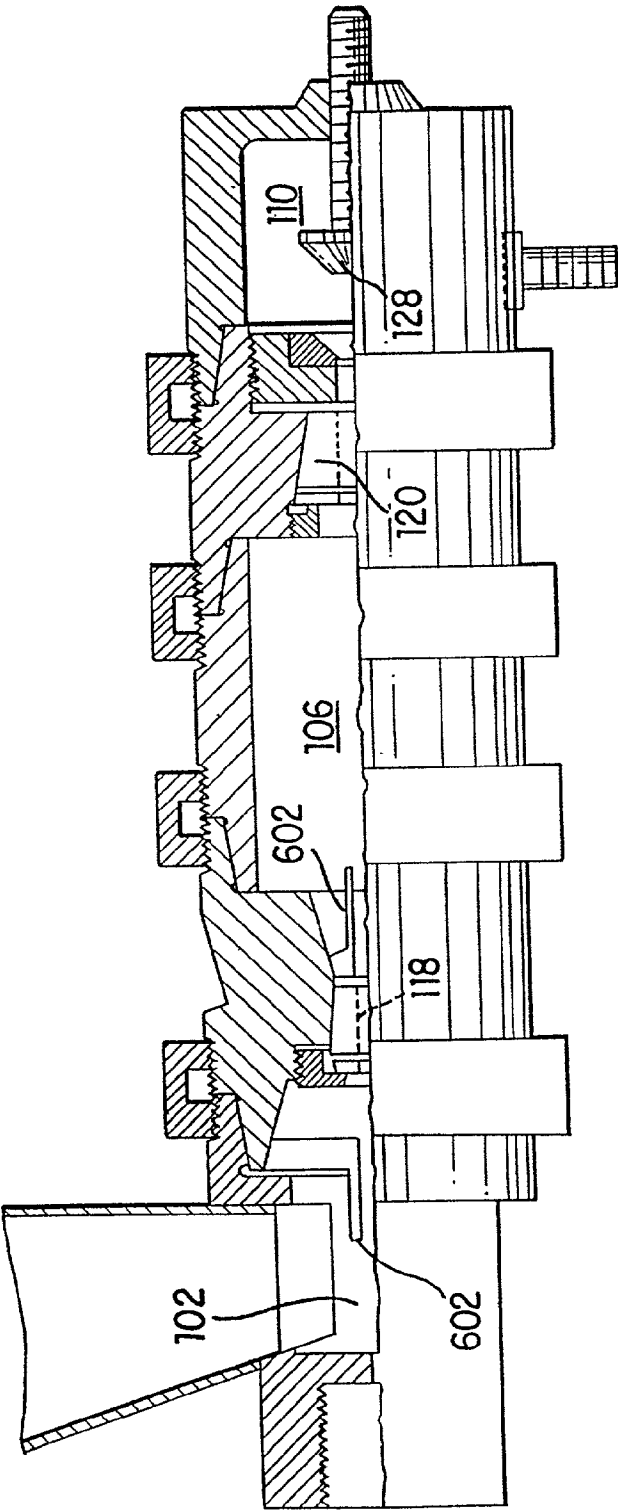


FIG. 6

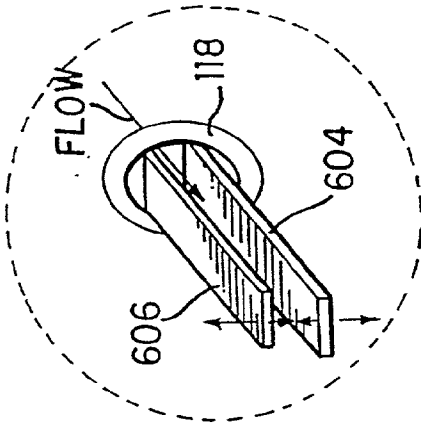
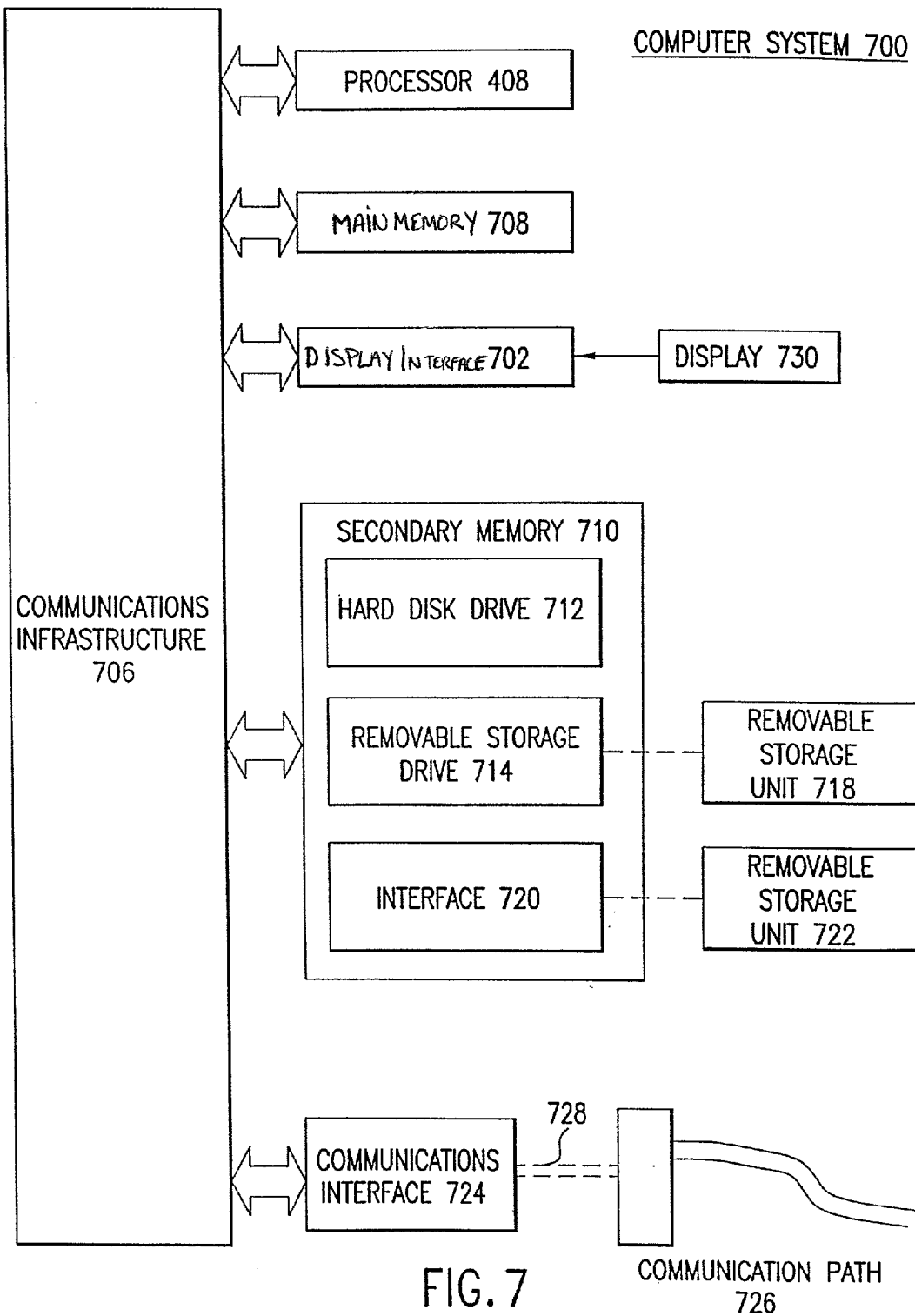
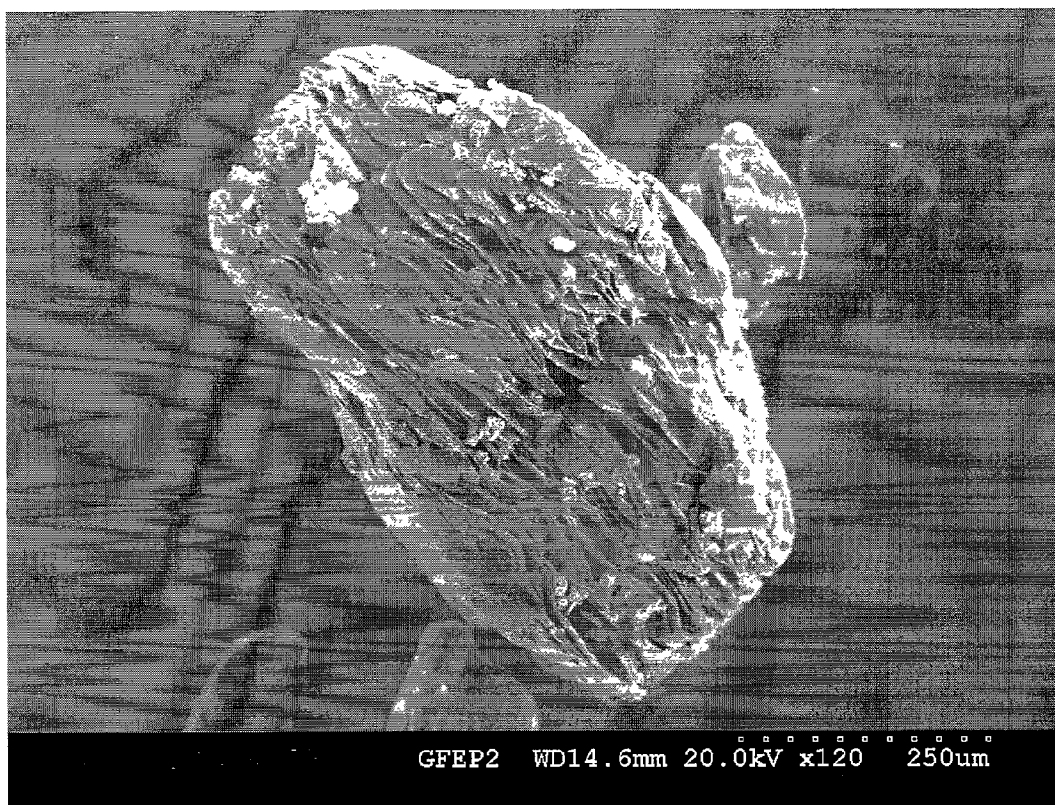


FIG. 6A





**FIG. 8**

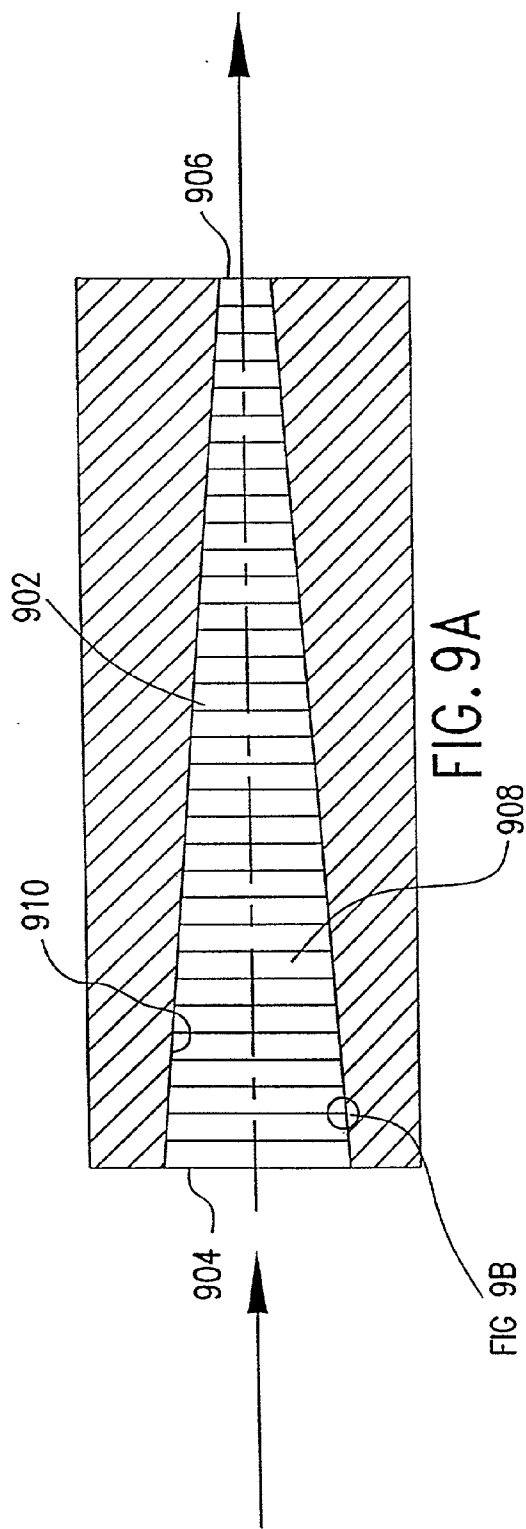


FIG. 9A

FIG. 9B

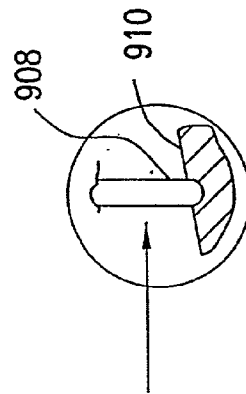


FIG. 9B

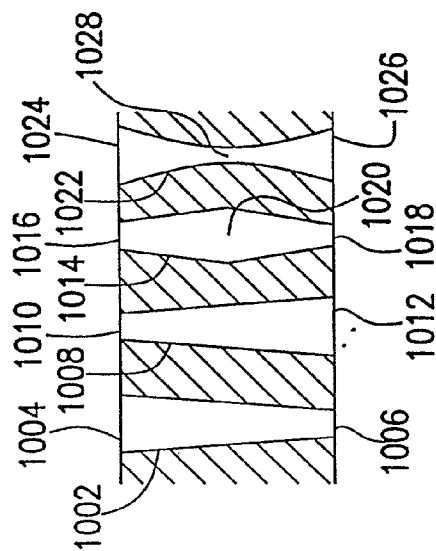
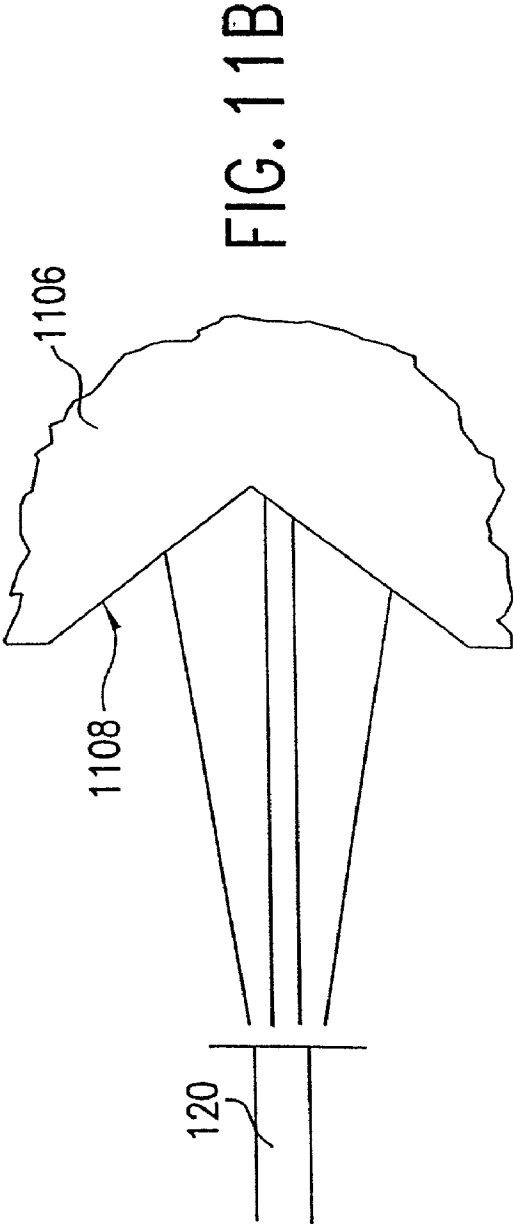
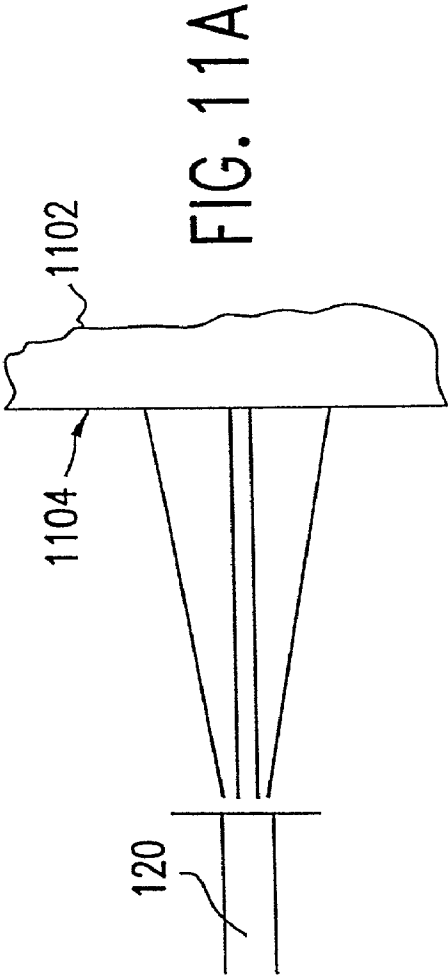


FIG. 10



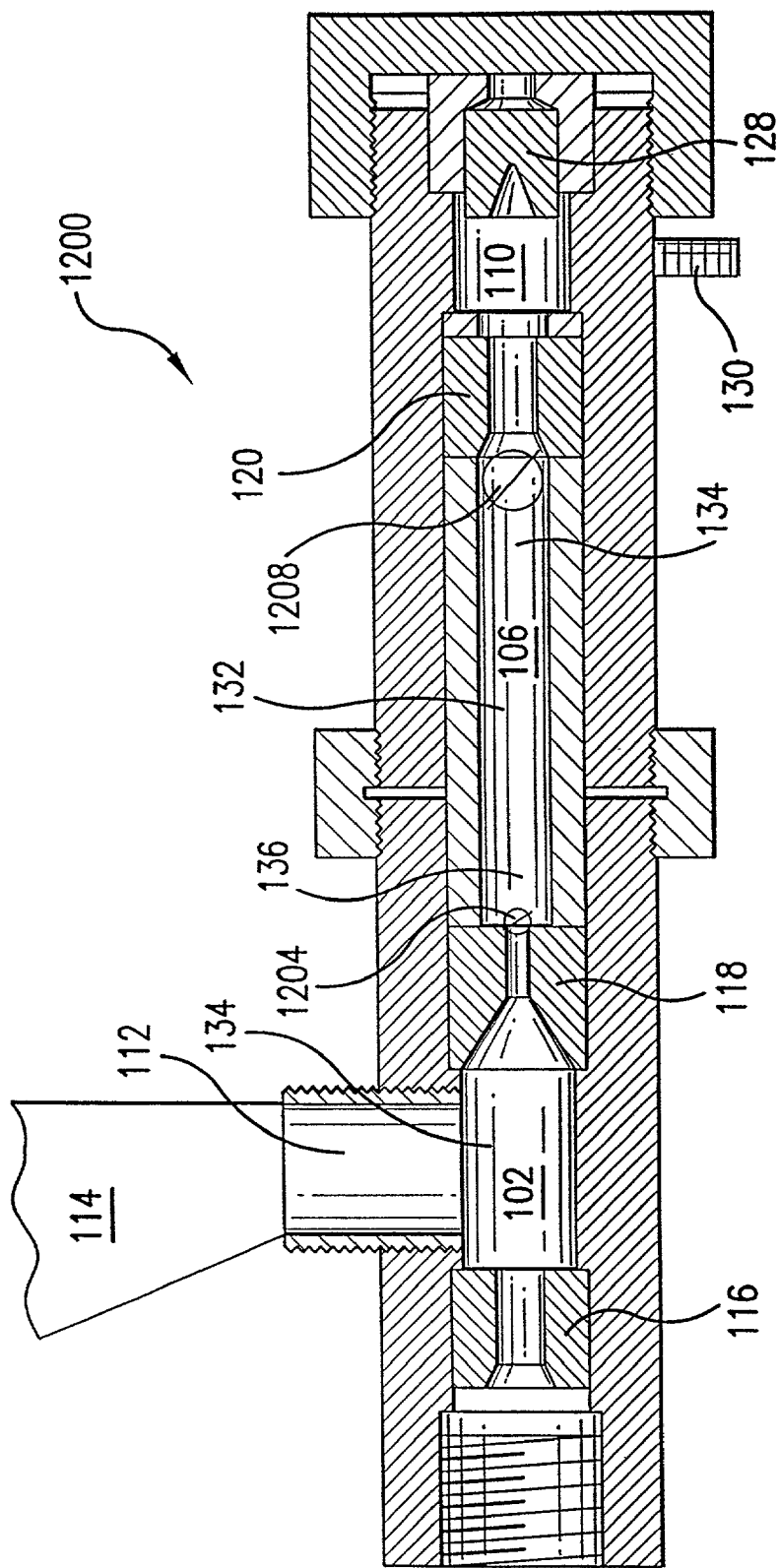


FIG.12

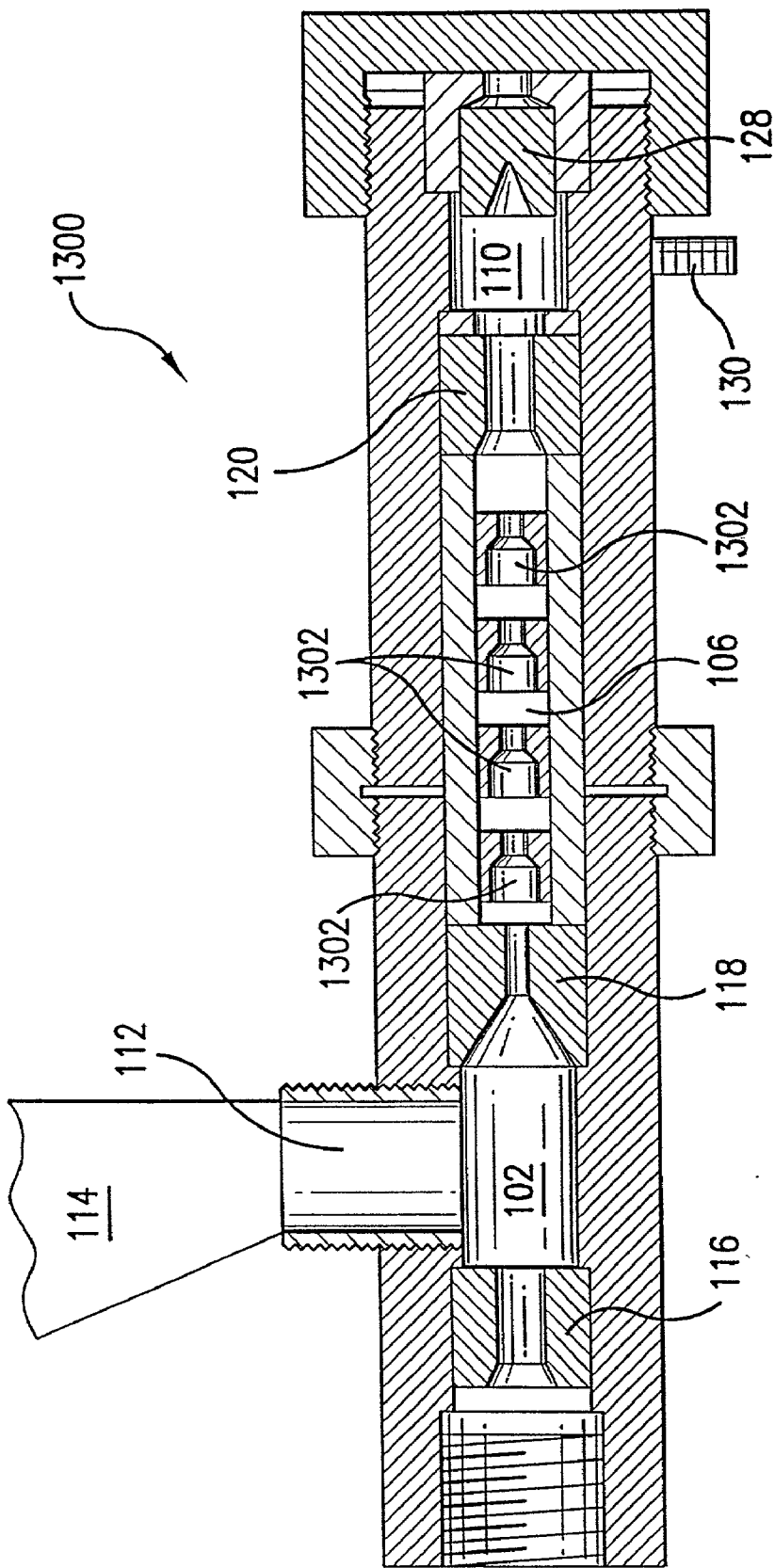
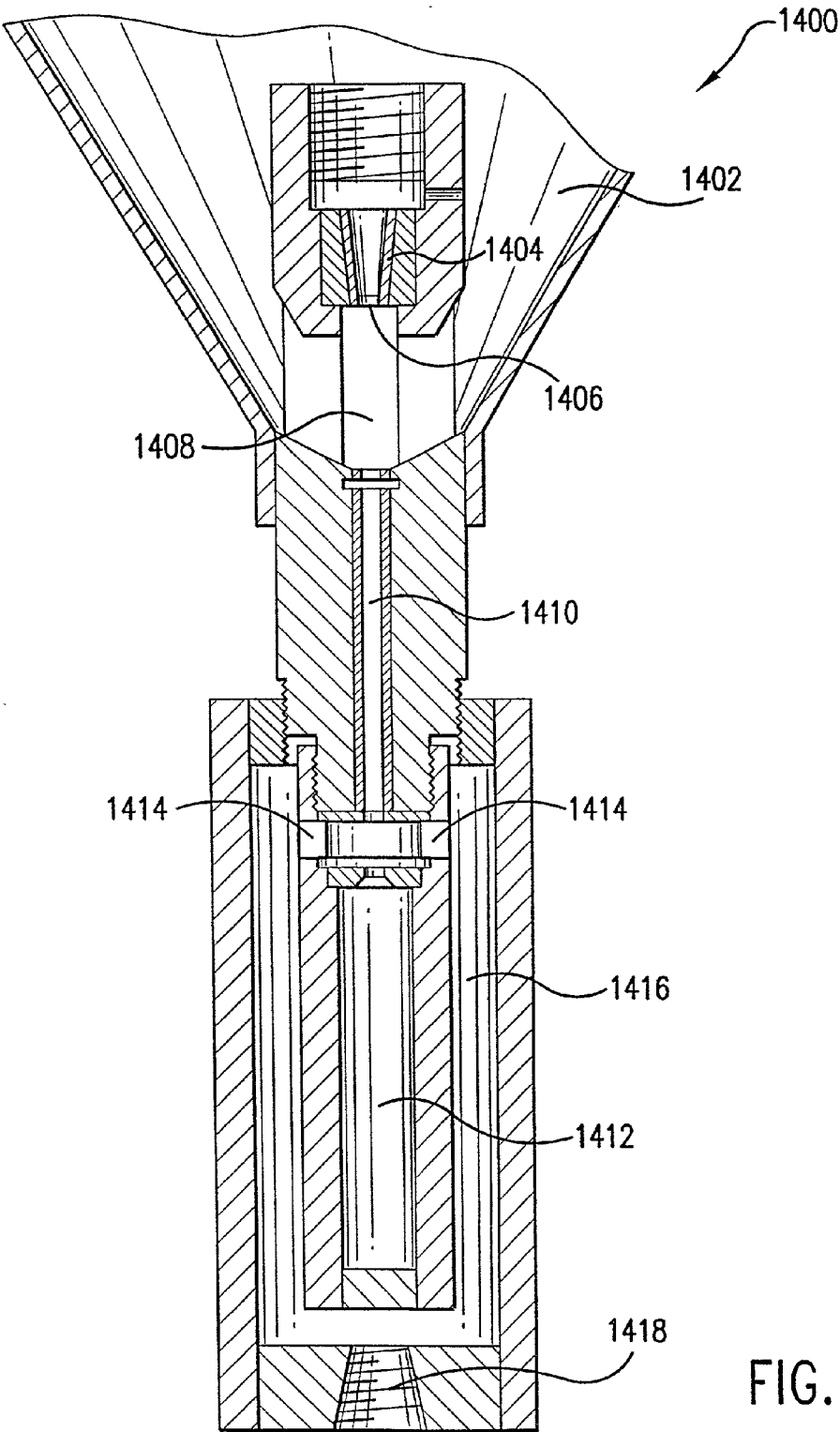
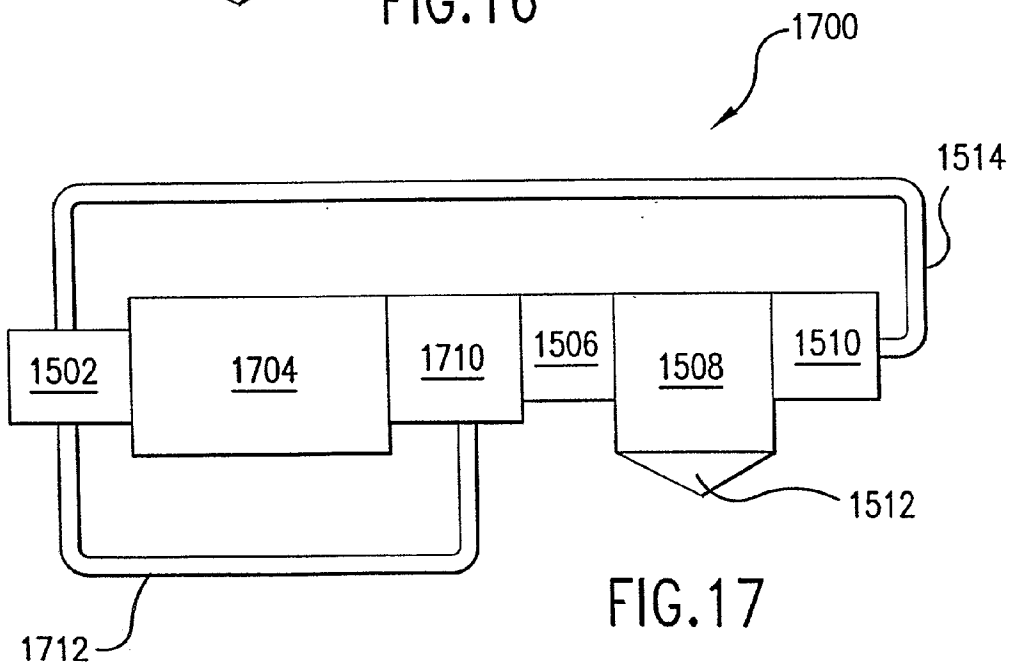
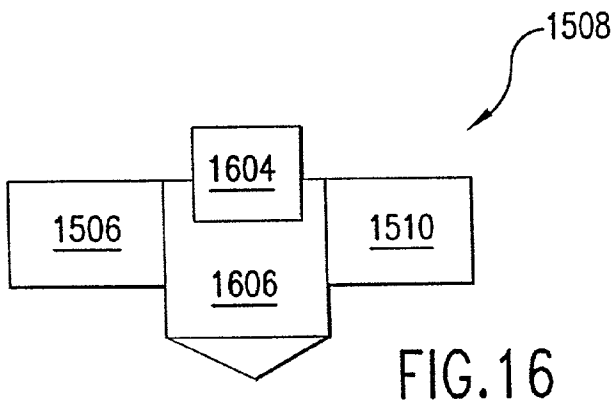
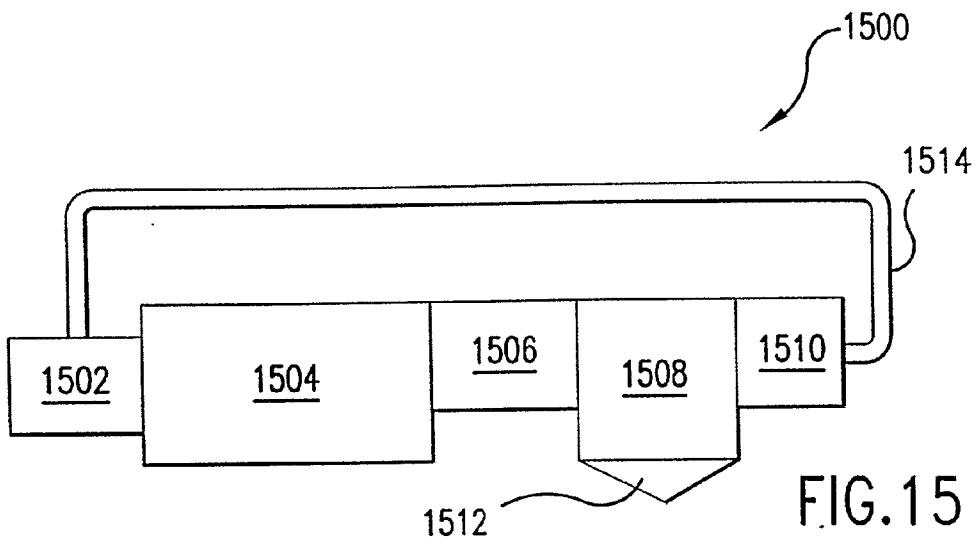
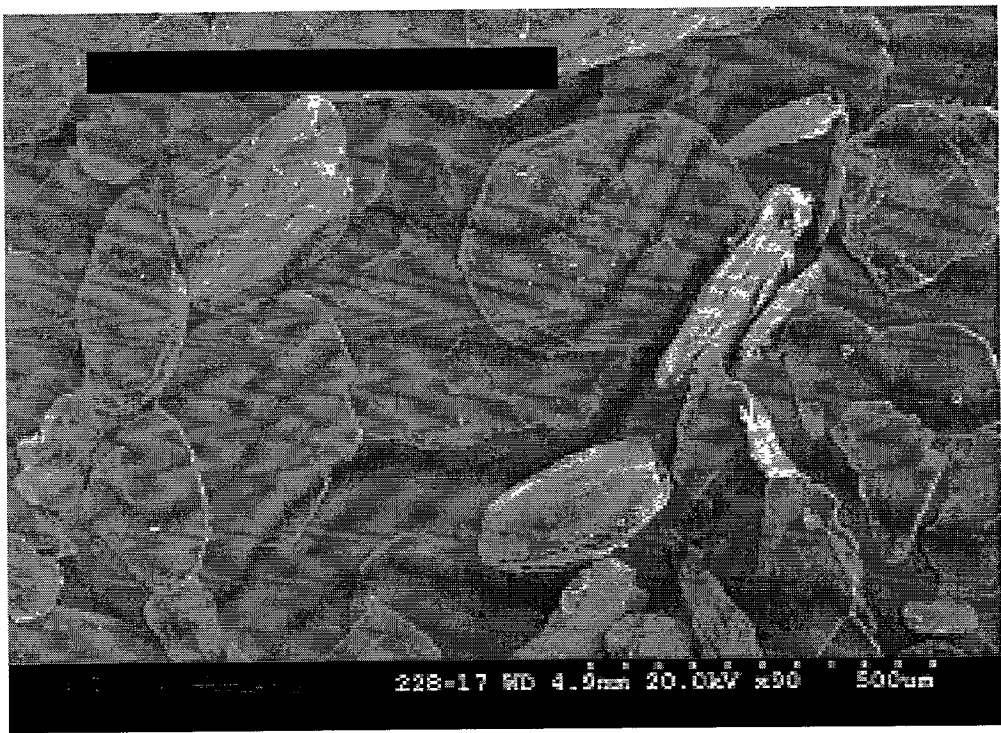


FIG.13









**FIG. 18**

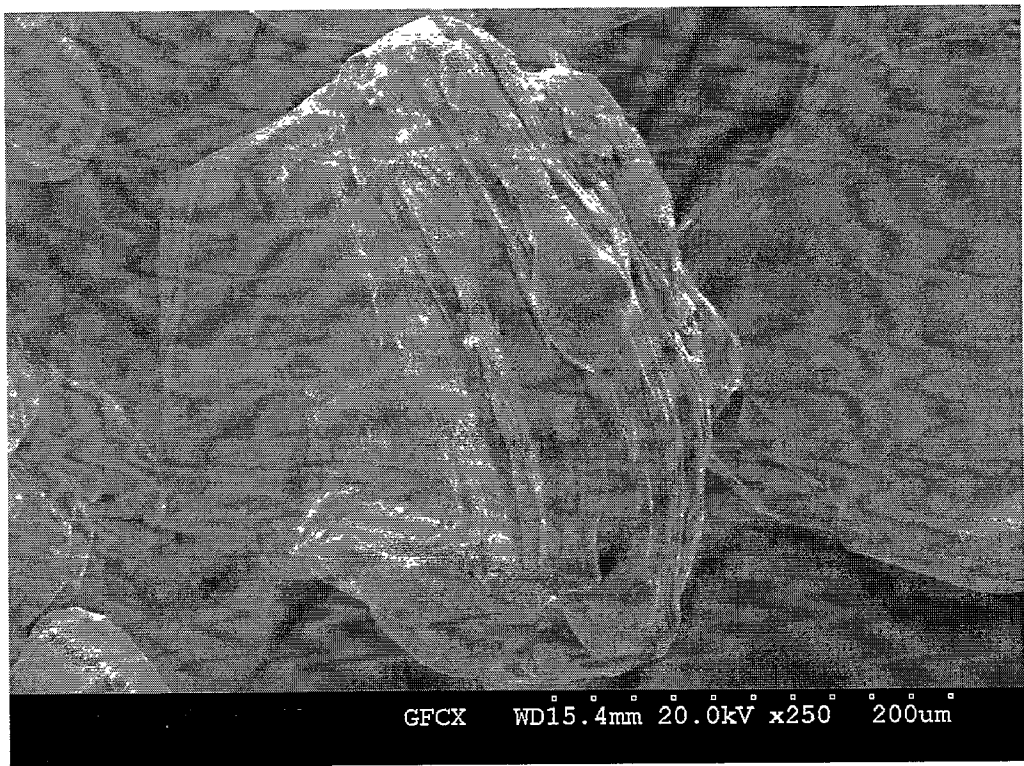


**FIG. 19**

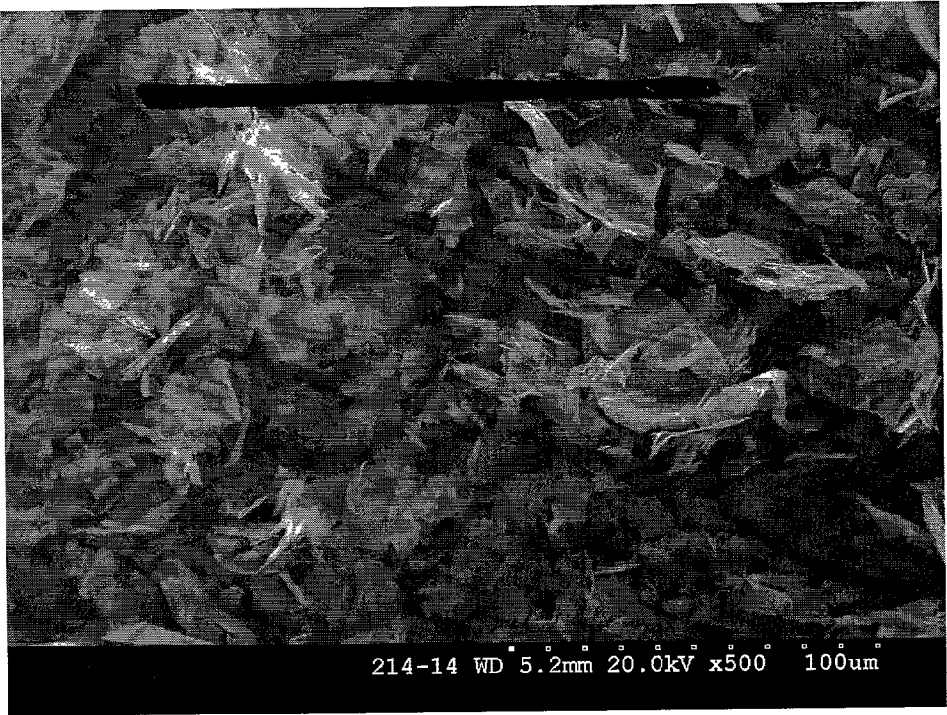


FIG. 20

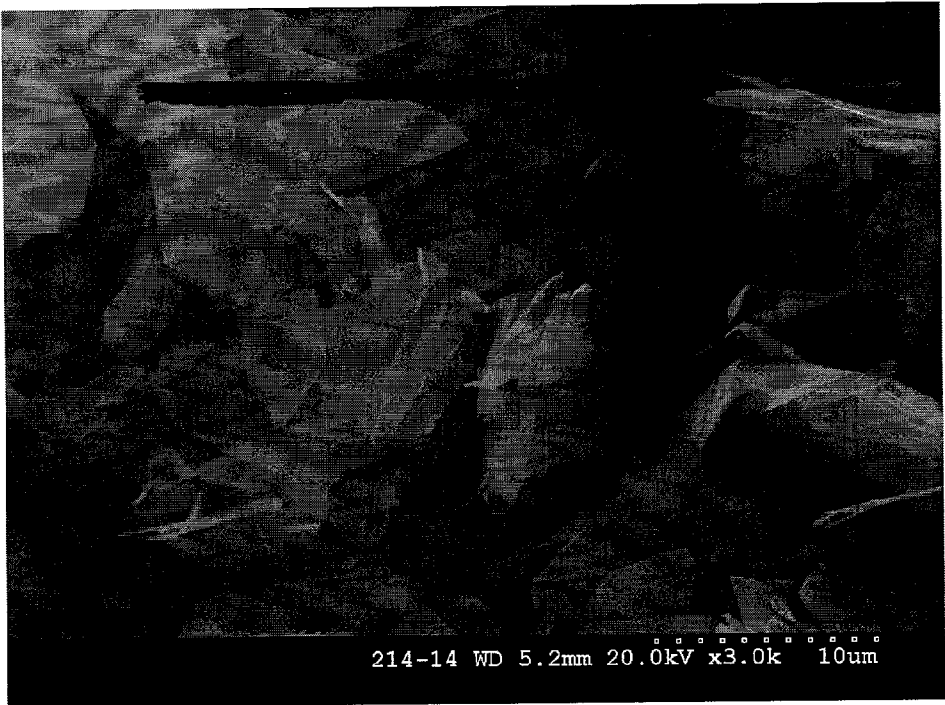


FIG. 21

## GRAPHITE PLATELET NANOSTRUCTURES

### BACKGROUND OF THE INVENTION

#### [0001] 1. Field of the Invention

[0002] The present invention relates generally to particle structures having a platelet-like appearance and a high aspect ratio. More particularly, the present invention relates to thin, independent graphite flakes or nanostructures having an aspect ratio of at least 1500:1 that are produced from graphite particles.

#### [0003] 2. Background Art

[0004] Graphite is used in a wide variety of applications, including, for example, industrial and automotive lubricants, specialty coatings (cathode ray tube coatings for conductivity and black matrix contrast, radiation absorbent coatings, battery can coatings, EMI shielding, etc.), bi-polar fuel cell separator plates, screen printable polymeric thick films (conductive and resistive), and fillers in a variety of polymer/plastic composites (such as polypropylene and nylon) for structural and electronic applications.

[0005] Currently, the majority of the uses cited above utilize expanded, or exfoliated, graphite or finely divided carbon black-type materials with high surface areas. Because graphite is a crystalline form of carbon, graphite comprises atoms bonded in flat, layered planes held together by bonds, or Van der Waals forces, between the planes. **FIG. 19** is a pictograph of raw crystalline graphite at a magnification of 250x. The graphite includes a number of layered planes, tightly packed and connected together to form a single particle.

[0006] Conventional manufacture of expanded graphite requires thermal and chemical treatment in order to expand the interlayers without completely breaking/separating the layers between the basal (hexagonal) planes. Typically, the expansion is conducted by treating particles of graphite, such as natural graphite flakes, with an intercalant, e.g., a solution of sulfuric and nitric acid, such that the crystal structure of the graphite reacts with the acid to form a compound of graphite and the intercalant. Upon exposure to elevated temperatures the particles of intercalated graphite expand in an accordion-like fashion in the c-direction, i.e., in the direction perpendicular to the crystalline planes of the graphite flakes. These elevated temperatures are usually above 700° C., and typically above 1000° C. The resulting expanded, or exfoliated, graphite particles are vermiform in appearance and are commonly referred to as "worms". An example of an expanded or exfoliated graphite structure is shown in **FIG. 18**.

[0007] This expansion of the particles into worms, rather than separation into separate platelets, occurs as a result of the Van der Waals forces securing together the basal planes of the graphite structure. The Van der Waals forces between the basal planes of the graphite prevent complete separation of the leaflets.

[0008] Expanded graphite structures may be used as particulate in composite materials, such as polymers, to provide reinforcement and add stiffness, strength and other properties. The use of such particulate-filled polymers in materials-intensive industries has almost quadrupled during the last two to three decades, especially in automotive applications.

Attractive benefits of the use of these polymers include low cost, weight reduction, styling potential, superior acoustic characteristics, reduced maintenance and corrosion resistance.

[0009] In most polymer composite applications, the resin system is mixed with expanded graphite, chopped fibers or other additives for processing and durability requirements and sometimes with fillers for further cost reduction. These additives are incorporated into the polymer or resin in specific amounts in order to customize properties of the resulting composite, such as stress, strain, impact strength and conductivity. Additionally, thermal, electrical, mechanical, chemical and abrasion properties are all affected by the form and matter of the particulate in polymers. Desired properties can be obtained or customized by varying filler content, matrix polymer type, and process techniques. However, the orientation and accommodation of the particulate in the component may cause weak areas, susceptible to crack initiation and propagation at sharp bends.

[0010] As components, particularly under the hood of automobiles, become more complex-shaped and miniaturized, particulate-filled polymers offer greater advantages over traditional polymer composites. In most cases, the reinforcements, additives, and fillers in polymers are relatively large scale particles, e.g., approximately 50  $\mu\text{m}$ , mainly due to the high cost and difficulties of producing finer particles. Thus, industrial commercialization has been limited for filled polymeric materials. Reasons for the limited use include: limits on performance and durability, including dimensional stability, creep and brittleness, and processing related problems, such as surface finish and paintability.

[0011] Some of these particulate-filled polymers are conductive polymers. Although almost all plastics, whether thermoplastic polymers or thermosetting polymers, are intrinsically good electrical insulators, introduction of graphitic and other carbonaceous materials into the polymers can create electrical conduction paths in the insulating polymer matrix when these particles contact each other above a certain content, or critical volume fraction.

[0012] Conductive polymers play an increasingly important role in very diverse industrial applications. Automotive components, CRT monitors, corrosion inhibitors and "smart" windows (capable of controlling sunlight intake) are examples of leading anti-static and other conductive properties utilized in newer product applications. The leading markets for traditional conductive polymers are fuel systems, business machines and wafer/chip handling devices.

[0013] Graphite, in general, can be used along with specially-processed electroconductive carbon black as a filler to provide electrical and thermal conductivity to normally non-conducting or poorly conducting polymeric materials. However, the size and morphological characteristics of conventional graphite particles limit the extent that the properties of a polymer composite can be improved.

[0014] Typical mainstream additives include specially-processed electroconductive carbon black, carbon fibers and metal (e.g., stainless steel) fibers.

[0015] The graphite and carbonaceous material conduction paths formed through polymers are dependent upon the decreasing particle size and resultant increasing dispersion, or packing density, of the filler in the matrix. The

critical volume fraction decreases with decreasing particle size. Once loading is achieved for a given particle size at the critical threshold ( $\phi_c$ ), the composite conductivity increases discontinuously as a function of this loading of filler, beyond which the particles form the necessary continuous conduction paths in the composites.

[0016] Metals are, by many orders of magnitude, more conductive than carbon black. Yet, carbon black is currently the filler of choice for most conductive polymeric applications. This is due to the small particle size and high surface area of carbon black. The grades of carbon black selected for use in conductive plastics are "high-structure" types consisting of long carbon chains with extensive branching, which occurs when primary particles of carbon black fuse together to form aggregates. These high-structure aggregates help form current paths through the plastic matrix. Powdered metals, on the other hand, typically are a large particle size, low in surface area and not structured. Because of these differences in physical form, some expensive specialty carbon blacks will impart conductive properties to some plastics at as low a concentration as 10%, while powdered metals may have to be used at concentrations as high as 80–90% by weight. Because of this, the price/performance difference between electroconductive carbon blacks and metals is formidable.

[0017] The development of enhanced graphite particles, having a structure that enables higher performance characteristics and mechanical properties would fulfill a number of fuel cell and automotive needs. For instance, the ability to manufacture low-cost, conductive, engineered plastic composites that are paintable and abrasion-resistant lowers automotive costs and allows greater use of polymeric composites in automobiles in environments not currently amenable to certain composites, such as under-the-hood parts and fuel cells.

#### BRIEF SUMMARY OF THE INVENTION

[0018] The present invention is separated graphite nanostructures formed of thin, independent graphite flakes or platelets. The nanostructures are shaped to have corners, or edges that meet to form points. The plates may be fully isolated from the original graphite particle, or may be partially attached to the original particle.

[0019] The graphite nanostructures have high specific surface area (the surface area of a particle reported as the surface area per gram). The graphite nanostructures have an average thickness in the range of 1 nm to 100 nm, but preferably in a range of about 5 nm to 20 nm. The graphite nanostructures also have a substantially planar surface area, or footprint, with geometrically irregular shapes having aerial dimension values within the range of 0.08  $\mu\text{m}$  to 100  $\mu\text{m}$ , preferably in the range of 10  $\mu\text{m}$  to 60  $\mu\text{m}$ , and more preferably in the range of 10  $\mu\text{m}$  to 40  $\mu\text{m}$ . The graphite nanostructures have a planar morphology with an aspect ratio calculated by dividing the average width or length dimension by the average thickness, substantially in the range of 1,500:1 to 100,000:1.

[0020] The graphite nanostructures can be added to conventional polymers to create polymer composites having improved mechanical and electrical characteristics, including increased flexural modulus, heat deflection temperature, tensile strength and electrical conductivity.

[0021] The graphite nanostructures are created from standard graphite using a high-pressure flaking mill. Fluid jets of the mill cause fluid to enter the tip of cracks in the graphite, which creates tension at the tip of the crack. This tension causes the cracks to propagate along the natural plane in the graphite so that small particles of the graphite separate into distinct flakes. As such, the mill provides a unique shape to these particles, viz, the natural smallest, planar particle of the graphite achievable.

[0022] The graphite nanostructures may be treated after the high-pressure flaking mill process by conventional drying technologies, including convection drying, freeze drying, spray drying, infrared drying and others. The flakes may also optionally be introduced into a hydrocyclone to separate the flakes by size. Also, the flakes may be recirculated back into the high-pressure flaking mill for further processing to either further thin the graphite nanostructures or to cleave the nanostructures to expose reactive inner surfaces of the graphite.

#### BRIEF DESCRIPTION OF THE FIGURES

[0023] The foregoing and other features and advantages of the invention will be apparent from the following, more particular description of a preferred embodiment of the invention, as illustrated in the accompanying drawings.

[0024] FIG. 1 shows a first embodiment of a high-pressure flaking mill for manufacturing the graphite platelets of the present invention.

[0025] FIG. 2 shows a cross-sectional view of a cavitating nozzle of the high-pressure flaking mill of FIG. 1.

[0026] FIG. 3 shows a second embodiment of a high-pressure flaking mill for manufacturing the graphite platelets of the present invention.

[0027] FIG. 4 shows a high-pressure flaking mill and data control system for manufacturing the graphite platelets of the present invention.

[0028] FIG. 5 shows an alternate embodiment of a third chamber of the high-pressure flaking mill for manufacturing the graphite platelets of the present invention in which an ultrasonically vibrating horn is used.

[0029] FIG. 6 shows an alternate embodiment of the high-pressure flaking mill for manufacturing the graphite platelets of the present invention in which one or more self-resonating elements are used.

[0030] FIG. 6A shows a detailed view of the self-resonating elements of FIG. 6.

[0031] FIG. 7 shows an exemplary computer system used to implement the high-pressure flaking mill and data control system for manufacturing the graphite platelets of the present invention.

[0032] FIG. 8 is a pictograph showing a traditionally-exfoliated graphite structure having a vermiform appearance, or a worm structure.

[0033] FIG. 9A shows an alternate embodiment of a slurry nozzle for manufacturing the graphite platelets of the present invention.

[0034] FIG. 9B shows an exploded view of an area of the slurry nozzle of FIG. 9A.

[0035] FIG. 10 shows alternate embodiments of slurry nozzles for manufacturing the graphite platelets of the present invention.

[0036] FIGS. 11A and 11B show alternate embodiments of a collider for manufacturing the graphite platelets of the present invention.

[0037] FIG. 12 shows an alternate embodiment of the high-pressure flaking mill wherein cavitation is created by electronically controlled valves.

[0038] FIG. 13 shows an alternate embodiment of the high-pressure flaking mill wherein cavitation is created by a series of nozzles.

[0039] FIG. 14 shows an alternate embodiment of the high-pressure flaking mill in a vertical configuration.

[0040] FIG. 15 shows an alternate embodiment of the high-pressure flaking mill including a spray dryer.

[0041] FIG. 16 shows an embodiment of a spray dryer equipped with a collector and condenser.

[0042] FIG. 17 shows another embodiment of FIG. 15, including a hydrocyclone.

[0043] FIG. 18 is a pictograph showing non-expanded, crystalline graphite at a magnification of 90x.

[0044] FIG. 19 is a pictograph showing conventional, raw, crystalline graphite at a magnification of 250x.

[0045] FIG. 20 is a pictograph showing the graphite nanostructures of the present invention at a magnification of 500x.

[0046] FIG. 21 is a pictograph showing the graphite nanostructures of the present invention at a magnification of 3000x.

#### DETAILED DESCRIPTION OF THE INVENTION

[0047] A preferred embodiment of the present invention is now described with reference to the figures where like reference numbers indicate identical or functionally similar elements. Also in the figures, the left most digit or digits of each reference number corresponds to the figure in which the reference number is first used. While specific configurations and arrangements are discussed, it should be understood that this is done for illustrative purposes only. A person skilled in the relevant art will recognize that other configurations and arrangements can be used without departing from the spirit and scope of the invention.

[0048] Graphite itself is a polymorph of the element carbon and its most stable form, with strong carbon-carbon bonds in a sheet-like structure wherein the atoms all lie in a plane and are only weakly bonded to the graphite sheets above and below. Graphite is a soft carbon, an excellent lubricant, and conductor of heat and electricity.

[0049] The present invention is separated, graphite nanostructures formed of thin, independent graphite flakes having an aspect ratio of at least 1500:1 that are produced from all types of synthetic and natural graphite particles. Each single platelet is a flaked graphitic layer consisting of multi-aromatic, carbon-ring nanostructures. The term

"nanostructures" is meant to include particles having at least one dimension that is less than one micrometer.

[0050] The graphite nanostructures have high specific surface area (the surface area of a particle reported as the surface area per gram) in the range of about 1.5 m<sup>2</sup>/g to 30 m<sup>2</sup>/g, but preferably in the range of about 5 m<sup>2</sup>/g to 25 m<sup>2</sup>/g, and more preferably in the range of 5 m<sup>2</sup>/g to 20 m<sup>2</sup>/g. The graphite nanostructures have an average thickness in the range of 1 nm to 100 nm, but preferably in a range of about 5 nm to 20 nm, and more preferably in a range of about 5 nm to 10 nm. The graphite nanostructures also have a substantially planar surface area, or footprint, of about 0.08  $\mu\text{m} \times 100 \mu\text{m}$ , but is preferably about 10  $\mu\text{m} \times 60 \mu\text{m}$ , and more preferably of about 10  $\mu\text{m} \times 40 \mu\text{m}$ . The nanostructures have a planar morphology with an aspect ratio substantially in the range of 1,500:1 to 100,000:1, but preferably substantially in the range of 1,500:1 to 20,000:1, and more preferably substantially in the range of 1,500:1 to 8,000:1.

[0051] The aspect ratio of the nanostructures is calculated by taking the largest dimension divided by the smallest dimension of an individual platelet. Typically, the smallest dimension is the thickness direction of each platelet, as it is generally in the nanometer range.

[0052] An aerial aspect ratio of individual nanostructures can also be calculated by finding an average length measurement divided by an average width measurement. For instance, an average of three width measurements divided by an average of three length measurements, where each measurement is taken at a different location across the platelet, to find an average diameter value. The aerial aspect ratio of the graphite nanostructure of the present invention is preferably in the range of 1 to 50, more preferably in the range of 2 to 25 and still more preferably in the range of 3 to 9. Average platelet dimensional values for the length and width measurements range from about 0.08  $\mu\text{m}$  to 300  $\mu\text{m}$ .

[0053] FIGS. 18 and 19 show photographs of crystalline graphite particles from which the nanostructures of the present invention are formed. Each graphite particle comprises many graphite layers bonded together to form the single particle. For comparison, FIGS. 20 and 21 show nanostructures magnified at 500x and 3000x, respectively. The nanostructures are characterized by a three-dimensional, separated structure of highly-conductive platelets. The nanostructures are substantially single-layered particles having large aspect ratios exceeding 1,500:1. Each flake may be separate from every other flake, so that each is an independent structure. Alternatively, the flakes may be partially attached to the original particle. When partially attached, the flakes appear as a conglomerate of plates extending in random directions.

[0054] The nanostructures have an angled geometric structure, meaning that the plates are shaped to have corners, or that edges meet to form points. This unique geometric structure is not obtained by graphite that has been exfoliated using conventional techniques, or that has been mixed or blended. Mixing or blending typically causes the edges and corners of graphite particles to wear and become rounded. Sharp corners and edges are beneficial because, among other reasons, the edges more easily create conduction paths when the nanostructures are combined into a polymeric material.

[0055] The aspect ratio of the graphite nanostructures is, to a certain degree, dependent on the process parameters and

composition of the high-pressure flaking mill used to produce the structures, described below. The nanostructure thickness, footprint, resultant aspect ratio and degree of flaking can be controlled without thermal and/or chemical means or specialty processes such as high temperature fuming processes that are typically utilized to produce carbon black. Therefore, these graphite nanostructures cannot be formed via thermal and/or chemical methods.

[0056] Additionally, the high-pressure flaking mill method used to manufacture the graphite nanostructures results in a matrix material that is darker than standard graphite, which provides better contrast in a resultant picture in CRT coating applications.

[0057] Graphite has become exceedingly useful in advanced composite structures and high temperature applications. However, use of graphite in polymer reinforcement and as a moldable material for precision parts is severely limited due to its particle size, nonuniformity, roughness, and handling properties. Furthermore, the high cost of graphite fiber and graphite components limits its broad adaptation. For instance, at present, the primary source of "graphite fiber" composites is polyacrylonitrile ("PAN") carbon fiber, which is relatively expensive, and which yields only 50% of its weight when converted into graphite and combined with epoxies and other thermosetting materials. The graphite nanostructures of the present invention can be manufactured at a much lower price and with a yield of over 95%.

[0058] The high-pressure flaking mill for flaking the graphite, described in detail below, generates a number of intensive effects that result in the penetration, pressurization, and ultimate flaking of the graphite. The resulting nanostructures have a thin, planar and "fluffy" graphite morphology with a high surface area, a nanoscale-thickness and a micron-size "footprint".

[0059] The high-pressure flaking mill of the present invention inexpensively generates large volumes (up to 3,000 pounds/hour per mill) of graphite nanostructure from common synthetic or natural-mined graphite. The high-pressure flaking mill can directly produce nanostructures from any type of synthetic or natural graphite, including: lump graphite, which is found in chunks in large veins; crystalline flakes; and amorphous, or microcrystalline graphite. Several different embodiments of the high-pressure flaking mill are now described with reference to FIGS. 1-7 and 9-17.

[0060] FIG. 1 shows a first embodiment of a high-pressure flaking mill 100 for processing graphite into plate-like nanostructures. High-pressure flaking mill 100 includes a first chamber 102, nozzle chambers 104 and 108, a second chamber 106, and a third chamber 110. In one embodiment, chambers 102, 106 and 110 each have a length (measured from inlet to outlet) in the range of 1-20 inches and a diameter in the range of 0.25-10 inches. However, it would be apparent to one skilled in the relevant art that various other sizes and configurations of chambers 102, 106 and 110 could be used to implement high-pressure flaking mill 100 of the present invention.

[0061] First chamber 102 includes an inlet 112. The material to be processed, usually mined graphite, is fed into first chamber 102 via inlet 112. In this embodiment, a funnel 114 is disposed above inlet 112 to facilitate loading of the

material to be processed into first chamber 102. In an alternate embodiment, inlet 112 could be connected to an outlet of another similar high-pressure flaking mill, so that the graphite particles exiting a first high-pressure flaking mill could be pumped into a second stage high-pressure flaking mill to achieve further flaking, or if desired, cleaving of the particles. The second stage high-pressure flaking mill could be designed with the same chambers and features as the first high-pressure flaking mill, however, the nozzle sizes would be smaller than the first high-pressure flaking mill to accommodate the reduced size of the graphite particles.

[0062] Alternatively, a recirculation line could be connected to inlet 112 and an outlet of high-pressure flaking mill 100 so that graphite nanostructures exiting high-pressure flaking mill 100 could be recirculated into inlet 112 to achieve further flaking, or if desired, cleaving of the particles

[0063] The entire interior of each chamber of high-pressure flaking mill 100 could be coated with a thin layer of a material. Preferably, the material used for the coating is made from a material with the same chemical composition as the material that is being processed. For example, when treating graphite, the interior surfaces of each chamber can be coated by thin, diamond layer, which creates a thin, durable coating that is hard and has the same chemical composition as graphite. The coating may be applied by a process called chemical vapor deposition, which is well known in the art of coatings, or any other coating process that would be apparent to one skilled in the relevant art. The purpose of the coating is to reduce potential contamination by the material of the high-pressure flaking mill construction. When the high-pressure slurry jets contact the interior surfaces of the high-pressure flaking mill, any material that is dislodged from the mill will have the same composition as the material being processed.

[0064] As the particles pass through the high-pressure flaking mill, the volume of fluid in the slurry increases, thereby decreasing the flaking effect of the fluid jets. As such, in another embodiment, the slurry exiting high-pressure flaking mill 100 could be processed in a centrifuge to eliminate the excess fluid and make the slurry more concentrated before it is recirculated or fed into the second stage high-pressure flaking mill, as described above. Alternatively, the graphite particles could be completely dried and reintroduced into high-pressure flaking mill 100 in a dry state. As another alternative, the graphite particles could be recirculated in a wet or dry state, either automatically through the recirculation line extending from the output port of high-pressure flaking mill 100 to the first chamber 102, or any subsequent chamber, or manually by removing the processed graphite from the output of high-pressure flaking mill 100 and reintroducing the graphite to the mill for further treatment.

[0065] In one embodiment, the material to be processed is graphite, having a starting size, also referred to as a feed size, of 600-1,200 microns. Although this is a preferable range for the feed size, the feed size could be less than 600 microns and could be as high as 0.5 inches for lump graphite.

[0066] It would be apparent to one skilled in the relevant art that high-pressure flaking mill 100 could be used to flake and process a variety of other materials, both organic and



inorganic, having various feed sizes. For example, the high-pressure flaking mill of the present invention could be used to process any of the following: mica; vermiculite; silicon dioxide; carbon black; zirconia; silica; barium titanate; wollastonite; titania; boron nitride; natural and synthetic clays; polymers; and any other brittle or inorganic material that needs to be split, flaked or further micronized.

[0067] In one embodiment, the material particles are dry as they are fed into first chamber 102. In another embodiment, the material particles could be fed into first chamber 102 as part of a slurry, e.g., a mixture of material particles and a fluid.

[0068] It would be apparent to one skilled in the relevant art that high-pressure flaking mill 100 could be used with a variety of fluids, such as water or oil. Preferably, a fluid used in the high-pressure flaking mill will be able to penetrate the microcracks in the material being treated. The ideal fluid for use in the high-pressure flaking mill has the following properties: low viscosity for penetrating the crack of the material to be processed; low boiling point (50° C. or 106° F.) for easier separation of the fluid and solid; non-toxic; and not harmful to the environment. An example of fluids meeting these requirements are certain perfluoro carbons, available from Minnesota Mining and Manufacturing Company (3M) of Maplewood, Minn. Other fluids that could be used in the high-pressure flaking mill include: water; oil; cryogenic liquids including cryogenic carbon dioxide; liquefied gases including liquid carbon dioxide and liquid nitrogen; alcohol; silicone-based fluids including perfluoro carbon fluids; supercritical fluids including carbon dioxide or inert gas such as xenon or argon in a supercritical state; or organic solvents.

[0069] First chamber 102 further includes a high-pressure fluid jet nozzle 116 that creates a fluid jet using a pump (not shown). Fluid jet nozzle 116 preferably creates a water jet, however, it would be apparent to one skilled in the relevant art that other fluids could also be used. The fluid jet generated by nozzle 116 is configured in first chamber 102 such that the jet of fluid exiting from fluid jet nozzle 116 impacts or collides with the material particles after they enter inlet 112 to effect the flaking and peeling of the material. The fluid flow throughout the high-pressure flaking mill caused by the various nozzles is preferably a constant or continuous flow or, alternatively, can be an intermittent flow. The pump for nozzle 116 is designed for a particular volume discharge and a particular pressure. In the example of processing graphite, the nozzle diameter is preferably in a range between 0.005 to 1 inches, and more preferably in the range of 0.005 to 0.060 inches. The nozzle diameter is directly related to the pressure of the fluid and the volume discharge generated by the pump. As such, the range of nozzle diameters described above is suitable for a pressure range of fluid that could be as high as 100,000-150,000 psi.

[0070] It would be apparent to one skilled in the relevant art that the nozzle diameter could be larger than the above-mentioned range, depending on the size of the pump used to create the available volume range for the fluid jet. As such, as the amount of pump pressure capable of being achieved increases, the diameter of the nozzle can be increased, in relation thereto, when the volume of the fluid supply is sufficient.

[0071] In this embodiment, the nozzle of high-pressure fluid jet nozzle 116 is configured to emit a jet of fluid in the

general direction of nozzle chamber 104. One or more fluid jet nozzles 116 can be disposed in first chamber 102. If more than one fluid jet nozzle 116 is used, the plurality of fluid jet nozzles can be arranged in a straight line through first chamber 102, thereby directing each jet of fluid toward nozzle chamber 104. In one embodiment, the fluid jets from the multiple nozzles are arranged so that the jets are emitted substantially in parallel to each other. In an alternate embodiment, the fluid jets are designed to converge with each other. As the jet(s) of fluid impact the graphite, the particles are broken into smaller particles, and the slurry, i.e., the combination of the smaller particles and fluid, is forced into nozzle chamber 104.

[0072] Nozzle chamber 104 includes a primary slurry nozzle 118. Primary slurry nozzle 118 creates a jet of the slurry, and delivers the slurry jet into second chamber 106. The jet created by slurry nozzle 118 is preferably a continuous jet, as discussed above. Primary slurry nozzle 118 further creates turbulence in second chamber 106, which causes the smaller particles of the material to interact with each other and peel and flake further. In one embodiment, primary slurry nozzle 118 has a diameter in a range of 0.010-1 inch, and preferably within a range of 0.010-0.250 inches. The size of nozzle 118 is directly related to the size of fluid jet nozzle 116. As such, as the size of fluid jet nozzle 116 increases, so does the resultant size of slurry nozzle 118.

[0073] In one embodiment, nozzle chamber 104 further includes a cavitation nozzle 122. Cavitation nozzle 122 is shown in further detail in FIG. 2. As shown in FIG. 2, cavitation nozzle 122 has a channel 202 through which high velocity fluid flows. Cavitation nozzle 122 further includes an inner pin 204. In use, a hydrodynamic shadow is created in front of inner pin 204 that creates a pocket in which the flow is not continuous. Evaporation occurs in this pocket which creates cavitation bubbles in the fluid as it exits cavitation nozzle 122.

[0074] Cavitation nozzle 122, as shown in FIG. 1, is disposed adjacent second chamber 106. As such, as the slurry is passed through primary slurry nozzle 118 and into second chamber 106, the cavitation bubbles from the fluid exiting cavitation nozzle 122 implode and generate a local shock wave initiated from the center of each collapsing bubble in the whole volume of second chamber 106. The shock wave acts on the particles in the slurry and causes them to comminute further. As such, the particle size of the material entering second chamber 106 via an inlet 124 is larger than the particle size as the particles exit second chamber 106 via an outlet 126.

[0075] A secondary slurry nozzle 120 is disposed in a nozzle chamber 108 adjacent outlet 126 of second chamber 106. Secondary slurry nozzle 120 creates a second jet of slurry as it passes through the nozzle. In one embodiment, the diameter of secondary slurry nozzle 120 is within a range of 0.010-1 inch, and preferably within a range of 0.010-0.250 inches. Again, as discussed above with respect to primary slurry nozzle 118, the size of secondary slurry nozzle 120 is also related directly to the size of the high-pressure fluid jet nozzle 116, and the flow exiting secondary slurry nozzle 120 is preferably continuous.

[0076] Various embodiments of slurry nozzles are shown in FIGS. 9A, 9B and 10. In particular, FIG. 9A shows an embodiment of a slurry nozzle 902 that has an inlet 904 and

an outlet **906**, where the diameter of inlet **904** is larger than the diameter of outlet **906**. Further, an inner surface **910** of slurry nozzle **902** has sharp edges **908** that project slightly out from the inner surface, as shown in further detail in **FIG. 9B**. In this embodiment, sharp edges **908** are formed as rings and are disposed at intervals around inner surface **910** of slurry nozzle **902**. As the particles travel through slurry nozzle **902**, they hit one or more of the sharp edges **908**, which causes further breakdown and flaking of the graphite particles.

[0077] **FIG. 10** shows various possible embodiments of channel design for the slurry nozzles used to create the particles of the present invention. In a first slurry nozzle **1002**, an inlet **1004** has a diameter larger than an outlet **1006**, similar to nozzle **902** of **FIG. 9A**. In a second design, slurry nozzle **1008** has an inlet **1010** with a diameter which is smaller than the diameter of its outlet **1012**. A third slurry nozzle **1014** has an inlet **1016** and an outlet **1018** of approximately the same diameter, however, the inner surface of nozzle **1014** gradually tapers out from inlet **1016** toward a center point **1020** and then gradually tapers back in from center point **1020** toward outlet **1018**. A fourth slurry nozzle **1022** also has an inlet **1024** and an outlet **1026** of approximately the same diameter. In this embodiment, the inner surface of nozzle **1022** gradually curves inwardly from inlet **1024** toward a center point **1028**, and then gradually curves back outwardly from center point **1028** to outlet **1026**. It would be apparent to one skilled in the relevant art that various other nozzle designs could also be used to create the particles of the present invention.

[0078] The slurry jet emitted from secondary slurry nozzle **120** is directed toward third chamber **110**. A collider **128**, which also could be referred to as a “stopper” or “energy absorber,” is disposed in third chamber **110** directly in the path of the slurry jet. Collider **128** can be a stable collider, such as the screw mechanism shown in **FIG. 1**. Alternatively, collider **128** could be an ultrasonically vibrating collider **502**, as shown in **FIG. 5**. Ultrasonically vibrating collider **502** can be configured to have a vibration within a range of up to 20,000 Hz or higher. In one embodiment, ultrasonic vibrating collider **502** is the XL2020 Generator, available from Misonix Incorporated, Farmingdale, N.Y. In either embodiment, the position of collider **128** within third chamber **110** is preferably adjustable so that the collider can function to restrict the flow out of secondary slurry nozzle **120** and into third chamber **110**. This flow restriction causes increased turbulence to occur in second chamber **106**, which further aids in the flaking and peeling of the particles.

[0079] Two embodiments of colliders are shown in **FIGS. 11A and 11B**. In the embodiment of **FIG. 11A**, collider **1102** has a front surface **1104**, which is the surface that the slurry impacts. In this first embodiment, front surface **1104** is flat. In this embodiment, the slurry exits nozzle **120** and collides with flat front surface **1104**. In a second embodiment shown in **FIG. 11B**, collider **1106** has a front surface **1108** that is concave in the shape of an inverted cone. In this embodiment, as the slurry exits nozzle **120** and collides with front surface **1108**, the concave shape causes the particles to bounce off and collide with each other and/or collide with other areas of front surface **1108** to thereby cause further flaking of the particles. It would be apparent to one skilled in the art that the front surface **1108** could be formed in a variety of concave-like shapes to cause the same effect. For

example, a hole could be formed in front surface **1108** to cause the particles to further peel and flake the graphite.

[0080] In either embodiment, the slurry jet from secondary slurry nozzle **120** directly collides with collider **128** to effect additional comminution and exfoliation of the particles of material in the slurry. As discussed above, collider **128** is preferably positionable at various distances away from secondary slurry nozzle **120**. This distance, *D*, is shown, for example, in **FIG. 5** and marked with reference number **504**. As the collider is moved closer to the flow of slurry exiting from slurry nozzle **120**, i.e., as *D* decreases, the flow becomes more restricted. This restricted flow causes turbulence in second chamber **106**, which assists with flaking of the particles in that chamber.

[0081] Although high-pressure flaking mill **100** is described with respect to **FIG. 1** as an example, high-pressure flaking mill **100** could be used to create the desired nanostructures without the use of cavitation nozzle **122**. An alternate embodiment of a high-pressure flaking mill **1200** is shown in **FIG. 12**. In this embodiment, electronically-controlled valves are used instead of a nozzle to create cavitation inside second chamber **106**. In particular, a first valve **1204** is disposed at an inlet to second chamber **106** and a second valve **1208** is disposed at an outlet to second chamber **106**. Cavitation can be induced in second chamber **106** by creating a pressure differential between the pressure in primary slurry nozzle **118** and the pressure in second chamber **106** of approximately 100:1. Depending on the distance *D* between collider **128** and secondary slurry nozzle **120**, the flow restriction may cause such a pressure differential, which will in turn cause cavitation to be induced in second **106**. Electronically-controlled valves **1204** and **1208** on the inlet and outlet of second chamber **106** are connected to pressure sensors **134**. These valves can be used to change the size of the valve orifice to maintain the pressure differential in second chamber **106**.

[0082] Third chamber **110** further has an outlet port **130** disposed at the bottom of the chamber. After the collision between the slurry and collider **128**, the slurry flows to the bottom of third chamber **110** and exits via outlet port **130**. The high-pressure flaking mill **100** of the present invention is designed to create graphite nanostructures having an average thickness in the range of 1-100 nm and an aspect ratio of at least 1,500:1.

[0083] In an alternate embodiment, the flaking of the graphite can be achieved using different combinations of the nozzles and chambers discussed above. For example, in one embodiment, graphite flaking can be achieved using only first chamber **102**, primary slurry nozzle **118** and third chamber **110**. In an alternate embodiment, flaking can be achieved using only first chamber **102**, secondary slurry nozzle **120** and third chamber **110**. In another embodiment, multiple nozzles can be used in lieu of primary slurry nozzle **118**. The use of multiple nozzles in any portion of high-pressure flaking mill **100** will create more turbulence in the chambers of the mill thereby further increasing the size reduction factor, i.e., the ratio of the feed size of the particles to the product size of the resultant particles, of the mill.

[0084] In a further embodiment, a self-resonating device **602**, as shown in **FIG. 6**, can be placed throughout high-pressure flaking mill **100**. In the embodiment shown in **FIG. 6**, beams **604** and **606** of self-resonating device **602**, shown



in FIG. 6A, are disposed at a certain distance apart from one another and configured to have a self-resonating frequency, such that the amplitude of the movement of beams 604 and 606 will contribute to the comminution and exfoliation process. It would be apparent to one skilled in the relevant art that two or more such beams could be positioned around a center line to create self-resonating device 602.

[0085] In the example shown in FIG. 6, self-resonating devices 602 are disposed in first chamber 102 and in front of primary slurry nozzle 118. However, it would be apparent to one skilled in the relevant art that these devices could be placed in a variety of locations in high-pressure flaking mill 100 to aid in flaking the graphite particles.

[0086] In one embodiment, high-pressure flaking mill 100 may be fitted with sensors to monitor the flaking process, as will be discussed in further detail below with respect to FIG. 4. For example, temperature sensors 132, pressure sensors 134, and sound sensors 136 may be disposed in various areas of each chamber of high-pressure flaking mill 100. By way of example, these sensors are shown placed in various positions within high-pressure flaking mill 100 in FIG. 1. For example, temperature sensors 132 are shown disposed in front of nozzle 116, in front of primary slurry nozzle 118, in second chamber 106, and in third chamber 110. Similarly, pressure sensors 134 are disposed in front of nozzle 116, in front of primary slurry nozzle 118 and in second chamber 106, and sound sensors 136 are disposed adjacent the inlet 124 and outlet 126 of second chamber 106. The pressure sensors 134, controlling the cavitation action in the chamber, can be linked to a centralized data control system 400. An embodiment of this data control system for the mill of the present invention will be discussed in further detail with respect to FIG. 4.

[0087] Temperature and pressure can be measured merely to collect data to keep track of the temperature ranges that occur during the graphite flaking process and to ensure that the pressure created by the various nozzles is sufficient to result in the graphite nanostructures. The sound is measured in second chamber 106 to obtain a reading of how intense the flaking process is in the cavitation chamber. In particular, the frequency of the sound that occurs in this chamber is measured. Typically, the frequency emitted depends on the conditions when cavitation is induced. Frequencies are generally within the range of 10-1000 KHz. In an alternate embodiment, high-pressure flaking mill 100 can be used in a production line to flake the graphite in mass volume. In such a case, the data from the sensors can be fed back to a computer-controlled mill to control the graphite flaking process.

[0088] Another embodiment of a high-pressure flaking mill 1300 is shown in FIG. 13. In this embodiment, cavitation is created in a second chamber 106 by a series of nozzles. Second chamber 106 is made up of multiple nozzles 1302 arranged in a series. The nozzles 1302 may be all the same size and shape or may be a variety of diameters and shapes. As the fluid flows through nozzles 1302, a pressure drop occurs in the larger diameter portion of each nozzle 1302. The sudden reduction in pressure causes cavitation bubbles to form, introducing cavitation into the flaking process.

[0089] Another embodiment of a high-pressure flaking mill 300 is shown in FIG. 3. High-pressure flaking mill 300

has a first chamber 302 and a second chamber 304 disposed on opposite ends of a third chamber 306. First chamber 302, similar to first chamber 102, has an inlet 308, a funnel 310, and a high-pressure fluid jet nozzle 312. As described previously in FIG. 1, as the graphite particles of the material travel down funnel 310 and enter first chamber 302 via inlet 308, the fluid jet from nozzle 312 collides or impacts with the particles, thereby breaking them apart and separating the particles into independent flakes or leaflets. The fluid jet nozzle 312 is oriented in first chamber 302 such that the slurry passes through first chamber 302 and into a nozzle chamber 320. Nozzle chamber 320 contains a first slurry nozzle 324. First slurry nozzle 324 creates a fluid jet of the slurry created in first chamber 302.

[0090] Similarly, second chamber 304 includes an inlet 314, a funnel 316, and a fluid jet nozzle 318. The same process occurs in second chamber 304 in which the particles travel down funnel 316 through inlet 314 and are impacted by a jet of fluid from nozzle 318. The slurry from second chamber 304 passes through to a nozzle chamber 322. Nozzle chamber 322 includes a second slurry nozzle 326, which creates a jet from the slurry produced in second chamber 304.

[0091] The jets from first and second slurry nozzles 324 and 326 are disposed such that they collide with each other in a high velocity collision within third chamber 306. This collision causes further breakdown and flaking of the particles. The slurry then falls to the bottom of third chamber 306 and exits via an outlet 328. Temperature, pressure and sound sensors, similar to those discussed with respect to high-pressure flaking mill 100 in FIG. 1, can also be used in high-pressure flaking mill 300 to acquire data and control the flaking process.

[0092] Another embodiment of a high-pressure flaking mill 1400 is shown in FIG. 14. High-pressure flaking mill 1400 is vertically configured and includes a primary nozzle 1404, a first chamber 1408, a secondary nozzle 1410, a catcher 1412, an overflow nozzle 1414, and an overflow channel 1416. Secondary nozzle 1410 could be a single nozzle, as shown, or could be multiple nozzles arranged in series as described and shown with reference to FIG. 13. The material to be peeled or flaked is fed into first chamber 1408. In this embodiment, a funnel 1402 facilitates loading of the material to be processed into first chamber 1408 and into the high-pressure flaking mill. As in a previous embodiment, the particles may be fed into the high-pressure flaking mill dry or as part of a slurry. Primary nozzle 1404 is a high-pressure fluid jet nozzle. The fluid from primary nozzle 1404 collides with the particles fed into first chamber 1408 from funnel 1402.

[0093] Primary nozzle 1404 is configured to emit a stream of fluid through the first chamber 1408 and through the secondary nozzle 1410. The secondary nozzle 1410 has a significantly larger diameter than primary nozzle outlet 1406 to allow the stream to flow through it. After the slurry flows through secondary nozzle 1410, it flows into the catcher 1412 through overflow nozzle 1414, where the churning action created by the fluid jet breaks down and peels the planar layers from the original graphite particles.

[0094] The use of the catcher 1412 in this embodiment rather than the collider 128 in the earlier discussed embodiment helps to prevent contamination by the material of the

collider. The jet formed by secondary nozzle **1410** and directed toward catcher **1412** allows the slurry from the catcher **1412** to exit back up through overflow nozzle **1414** as catcher **1412** fills and overflows. The slurry escapes through a space in the periphery of nozzle **1410**. The amount and rate of outflow from the catcher **1412** can be controlled by adjusting the size of overflow nozzle **1414**. As a result, the amount of flaking of the particles can be increased or decreased by adjusting the amount of time the particles are held in catcher **1412**.

[0095] After the slurry backflows through overflow outlet **1414**, it flows through the periphery of nozzle **1410** and into an overflow channel **1416** where it exits high-pressure flaking mill **1400** through outlet port **1418**.

[0096] Other embodiments of the high-pressure flaking mills described include a hydrocyclone and/or a spray dryer. A specific embodiment is shown in FIG. 15, where system **1500** includes a high pressure pump **1502**, connected to a high-pressure flaking mill **1504**. High-pressure flaking mill **1504** has attached a feed pump **1506** for introducing the graphite nanostructures into a spray dryer **1508**. Connected to spray dryer **1508** is a condenser **1510** and a collector **1512**. A recycling circuit **1514** connects condenser **1510** to high pressure pump **1502**. However, it would be apparent to one skilled in the relevant art that various configurations of these elements could be used to implement system **1500**. High-pressure flaking mill **1504** outputs a slurry containing the graphite nanostructures and the energy transfer fluid. If an additive, such as a polymer resin, was introduced into the high-pressure flaking mill, along with the graphite, the output will include the nanostructure material, the energy transfer fluid and the additive. As would be apparent to one skilled in the relevant art, the material and the additive could be comprised of more than one material or additive.

[0097] As stated above, the ideal fluid has the following properties: low viscosity for penetrating the crack of the material to be processed; high density for better impaction; low boiling point (50° C. or 106° F.) for easier separation of the fluid and solid; non-toxic; and not harmful to the environment. An example of fluids meeting these requirements are certain perfluoro carbons, water; oil; cryogenic liquids including cryogenic carbon dioxide; liquified gases including liquid carbon dioxide and liquid nitrogen; alcohol; silicone-based fluids including perfluoro carbon fluids; supercritical fluids including carbon dioxide or inert gas such as xenon or argon in a supercritical state; or organic solvents.

[0098] As shown in FIG. 16, spray dryer **1508** is attached to feed pump **1506**, and is comprised of atomizing components, such as a nozzle **1604** and a heating chamber **1606**. Typically, a spray dryer mixes a spray and a drying medium, such as air, to efficiently separate the graphite nanostructures from the fluid as the particles fall through the air.

[0099] There are four general stages to spray drying: atomizing, mixing, drying, and separation. First, the feed or slurry is atomized into a spray. This is accomplished by introducing the slurry to feed pump **1506**, which forces the slurry through atomizing nozzle **1604**. The energy required to overcome the pressure drop across the nozzle orifice is supplied by feed pump **1506**.

[0100] Second, the spray is mixed with a drying medium, such as air. Air can be added through a blower via nozzle

**1604**, via an additional nozzle, or can be merely present in chamber **1606**. As would be apparent to one skilled in the relevant art, other drying mediums could be introduced in spray dryer **1508**. For instance, because graphite is oxygen sensitive, inert gases such as nitrogen can be introduced as the drying medium. If a gas is added through a blower, the gas can be injected into chamber **1606** simultaneously with the atomized slurry. A conventional method of introducing gas and slurry simultaneously uses concentric nozzles, where one nozzle introduces gas and the other nozzle introduces slurry.

[0101] Third, the spray is dried. Drying occurs as the atomized spray, containing the graphite nanostructures, is subjected to a heat zone in chamber **1606** or, alternatively, a hot gas, such as air or an inert gas as described above, is injected into chamber **1606**. Flash drying quickly evaporates the fluid from the slurry, leaving only the dry graphite nanostructures. The small size of droplets allows quick drying, requiring a residence time in the heat zone ranging from 1-60 seconds, depending on the application. This short residence time permits drying without thermal degradation of the solid material.

[0102] Fourth, the product is separated from the gas. As the graphite nanostructures continue to fall, they exit chamber **1606**, accumulating in particle collector **1512**, located at the bottom of chamber **1606**. The now vaporized fluid is exhausted, or alternatively, collected in condenser **1510**. The spray dryer by-products are vaporized fluid and dry particles.

[0103] Using a spray dryer in connection with a high-pressure flaking mill provides several advantages over conventional drying techniques. For instance, spray drying produces an extremely homogeneous product from multi-component solids/slurries. A spray dryer can evaporate the energy transfer fluid from the slurry, leaving an additive, if used, and the nanostructure material. If the additive is a fluid, drying temperatures are held below the degradation temperature of the binder. As the energy transfer fluid evaporates, a very thin coating of binder polymerizes on each nanostructure. After being dried in the spray dryer, the particles are sufficiently coated for molding into compacts for sintering. Additional processing is not necessary.

[0104] Furthermore, the resulting collected nanostructures are fine, dry and fluffy. Conventional techniques, such as boiling the vapor off the particles, leave clumpy conglomerates of particles and result in less thorough blending of additives. The spray dryer also dries particles much faster than drying by conventional techniques. A spray dryer quickly dries a product because atomization exposes all sides of the particles to drying heat. The particles are subjected to a flash dry, and depending on the application, can be dried anywhere between 3 and 40 seconds. Thus, heat sensitive particles can be quickly dried without overheating the particles. As drying begins, the vaporized fluid forms around the particle. This "protective envelope" keeps the solid particle at or below the boiling temperature of the fluid being evaporated. As long as the evaporation process is occurring, the temperature of the solids will not approach the dryer temperature, even though the dryer temperature is greater than the fluid evaporation temperature.

[0105] An additional advantage is that the spray dryer can operate as part of a continuous process providing dry

particles as they are collected, rather than having to collect particles and then dry them. This also allows for fast turn-around times and product changes because there is no product hold up in the drying equipment.

[0106] The volume of an acceptable chamber 1606 can be determined by the equation, (residence time)\*(volume flow rate)=volume of chamber, where conditions of  $0 < a \leq 3$ ,  $0 \leq b < 3$ ,  $2 < a+b \leq 3$ ,  $0 < c \leq 4$ ,  $0 \leq d < 4$  and  $3 \leq c+d \leq 4$ . per unit mass, finer particles normally require longer residence time to dry than larger particles. Therefore, residence time may be longer for the finer materials. Increased temperature may also be used to accelerate drying of such materials.

[0107] The spray dryer can be used for drying any slurry, whether the slurry is comprised of graphite nanostructures, an additive, and an energy transfer fluid or comprised of only nanostructures and an energy transfer fluid. Further, the spray dryer can be a standard spray dryer, known in the art of spray drying. Spray dryer manufacturers and vendors include companies such as U.S. Dryer Ltd. of Migdal Ha'emek, Israel, Niro, Inc. of Columbia, Md., APV of Rosemont Ill., and Spray Drying Systems, Inc. of Randallstown, Md.

[0108] An additive, introduced into the high-pressure flaking mill can coat the graphite nanostructures as they are created. Accordingly, after drying, the outer surface of each nanostructure, or small conglomerates of nanostructures is partly or fully covered by a fine layer of the additive. In one embodiment, the additive is a thermoplastic. The thermoplastic coats the exterior surface of the nanostructure, creating a non-dusting nanostructure powder. As such, it is not as dusty or messy as uncoated graphite, and can be handled without leaving the same degree of graphite residue.

[0109] A conventional spray dryer can be outfitted with condenser 1510. Because all drying takes place in an enclosed chamber 1606, capture and condensation of the vapors is easily performed. Condenser 1510 collects the vaporized fluid from chamber 1606 and allows the spent fluid to be recovered. Thus, spray drying offers a simple way to contain the vapors from the evaporated fluid. Fluid recycling circuit 1514, as shown in FIG. 15, can connect condenser 1510 to high pressure slurry pump 1502 located at the first chamber of the high-pressure flaking mill. This allows condensed fluid to be recycled by returning the used fluid from the spray dryer to the high-pressure flaking mill. This reduces waste and contains the fluid, which is especially important when the fluid is a regulated product, such as isopropanol. Isopropanol can be used as the fluid in the high-pressure flaking mill, introduced into the spray dryer where it is vaporized, recondensed in the condenser and returned to the high-pressure flaking mill for reuse. In this way, the fluid vapors are contained without risk of releasing harmful vapors into the atmosphere.

[0110] If the fluid is water, the water can be released from the spray dryer as vapor, can be condensed to be discarded, or can be recycled through the fluid recycling circuit. As described above, a variety of fluids could be used as the energy transfer fluid in the high-pressure flaking mill.

[0111] In another embodiment, the slurry is introduced from the high-pressure flaking mill directly into the spray dryer. This embodiment does not use a feed pump connected to the nozzle for atomizing. Instead, fluid restrictors are used

at the high-pressure flaking mill outlet port to maintain the high pressures in mill 100. The slurry bypasses feed pump 1506 and is injected directly from the outlet of high-pressure flaking mill 100 into spray dryer 1508. In order to achieve proper separation of particles and fluid in spray dryer 1508, the slurry jet at the outlet of high-pressure flaking mill 100 must have sufficient speed to enter dryer 1508 to achieve complete atomization of the slurry. By eliminating the need for a feed pump to introduce the slurry to the spray dryer, the system operates more economically.

[0112] FIG. 17 shows another embodiment of system 1700 for processing graphite into nanostructures. This embodiment includes a hydrocyclone 1710 located between high-pressure flaking mill 1704 and feed pump 1506. In this embodiment, high-pressure flaking mill 1704 is the same configuration as high-pressure flaking mill 100. Hydrocyclone 1710 could also be incorporated in any of the other mill embodiments disclosed herein. Hydrocyclone 1710 can be located either before or after feed pump 1506, but is preferably located before it. A second feed (not shown) can be used to introduce slurry from high-pressure flaking mill 1704 to hydrocyclone 1710, or, the slurry can be introduced into hydrocyclone 1710 directly from high-pressure flaking mill 1704, as shown in FIG. 17.

[0113] Hydrocyclone 1710 aids in classifying solid particles exiting high-pressure flaking mill 1704 by separating very fine particles from coarser particles. The coarser particles are fed through a recycling line 1712 back into high pressure slurry pump 1502, to be reintroduced into high-pressure flaking mill 1704 for further processing. As the particles are still under pressure from hydrocyclone 1710, recycling line 1514 is a tube or enclosed circuit, which transfers the particles to high-pressure flaking mill 1704.

[0114] The slurry from high-pressure flaking mill 1704 enters the hydrocyclone 1710 at high velocity through an inlet opening and flows into a conical separation chamber. As the slurry swirls downward in the chamber, its velocity increases. Larger graphite structures are forced against the walls, dropped to the bottom, and discharged through a restricted discharge nozzle into recycle line 1712. The spinning forms an inner vortex which lifts and carries the finer particles up the hydrocyclone 1710, before they exit the discharge nozzle, and propel them through a forward outlet to feed pump 1506 or, alternatively, directly to spray dryer 1508.

[0115] In another embodiment, hydrocyclone 1710 is a dry-type cyclone, located after spray dryer 1508. In this embodiment, the graphite nanostructures are dried in spray dryer 1508 and gathered in collector 1512. The dry particles are introduced from collector 1512 into cyclone 1710, where the particles are sorted according to size. Cyclone 1710 operates substantially similar to the hydrocyclone described above, using a gas as the fluid. Again, oversized particles are reintroduced into high-pressure flaking mill 1704 or high pressure slurry pump 1502 via recycling line 1712. Because gases normally have less surface tension than fluids, dry separation normally results in finer and more accurate size distribution.

[0116] Hydrocyclone 1710 can be a commercially available hydrocyclone used for classification, clarification, counter-current washing, concentration, etc., of particles. Examples of hydrocyclone and cyclone manufactures are

Warman International, Inc. of Madison, Wis. (CAVEX® Hydrocyclone Technology), Polytech Filtration Systems, Inc., of Sudbury, MA (POLYCLON® Hydrocyclone Technology), and Dorr-Oliver, Inc., of Milford, Conn. (DORCLONE® HYDROCLONES).

[0117] Because hydrocyclone 1710 recycles the larger or more coarse fraction of material back to high-pressure flaking mill 1704 for further flaking, hydrocyclone 1710 assists in achieving a narrow size distribution of finished graphite nanostructures. Furthermore, hydrocyclone 1710 offers more intimate mixing of the graphite nanostructures and additives. Residence time in hydrocyclone 1710 is typically short, and is a function of the processing rate, and the equipment size (volume). Thus, residence time=equipment volume/processing rate (volume/time). Typically, the residence time in hydrocyclone 1710 is less than 60 seconds, and is preferably from 2-50 seconds. Thus, use of hydrocyclone 1710 does not restrict the processing rate achievable in high-pressure flaking mill 1704 and subsequent spray dryer 1508.

[0118] Depending on the size and capability of the hydrocyclone, residence time will vary for a given processing rate. Therefore, a properly sized hydrocyclone must be used to efficiently process graphite nanostructures. An improperly sized hydrocyclone could impose limits on the residence times in other components of system 1700.

[0119] FIG. 4 shows a high-pressure flaking mill and data control system 400 for use with the mill for manufacturing the nanostructures of the present invention. The high-pressure flaking mill of system 400 is similar to high-pressure flaking mill 100 in that it includes a first chamber 102 in which particles are impacted by a high-pressure fluid jet generated by nozzle 116, a nozzle chamber 104, a second chamber 106 in which cavitation occurs, a second nozzle chamber 108, and a third chamber 110 in which the graphite particles impact a collider for further breakdown and flaking.

[0120] Temperature sensor 132, pressure sensor 134 and sound sensor 136 are shown disposed in second chamber 106 of high-pressure flaking mill 100. In one embodiment, sensors 132, 134 and 136 are implemented using various transducers, thermocouples and user input, as would be apparent to one skilled in the relevant art.

[0121] Data collected by each of these sensors are fed into a signal conditioning module 402. In one embodiment, signal conditioning module 402 is a signal conditioner/isolator available from Omega Engineering, Stamford, Conn. Signal conditioning module 402 converts the signals transmitted from the sensors 132, 134 and 136 into a computer-readable format and passes them to data acquisition (DAQ) card 404. In one embodiment, DAQ card 404 is a data acquisition card available from National Instruments Corporation, Austin, Tex. The DAQ card 404 can be inserted or disposed in a PCMCIA slot 406 of a processor 408. Processor 408 processes the signals to acquire data regarding the comminution and exfoliation process. In one embodiment, processor 408 is running Lab View software that enables the user to view, store and/or manipulate the data received from the sensors to be used as control parameters in the control system.

[0122] It would be apparent to one skilled in the relevant art that the high-pressure flaking mill used to manufacture

present invention may be implemented using hardware, software or a combination thereof and may be implemented in a computer system or other processing system. In fact, in one embodiment, the invention is directed toward one or more computer systems capable of carrying out the functionality described herein. An example of a computer system 700 is shown in FIG. 7. The computer system 700 includes one or more processors, such as processor 408. Processor 408 is connected to a communication infrastructure 706 (e.g., a communications bus, cross-over bar, or network). Various software embodiments are described in terms of this exemplary computer system. After reading this description, it will become apparent to a person skilled in the relevant art how to implement the invention using other computer systems and/or computer architectures.

[0123] Computer system 700 can include a display interface 702 that forwards graphics, text, and other data from the communication infrastructure 706 (or from a frame buffer not shown) for display on the display unit 730.

[0124] Computer system 700 also includes a main memory 708, preferably random access memory (RAM), and may also include a secondary memory 710. The secondary memory 710 may include, for example, a hard disk drive 712 and/or a removable storage drive 714, representing a floppy disk drive, a magnetic tape drive, an optical disk drive, etc. The removable storage drive 714 reads from and/or writes to a removable storage unit 718 in a well-known manner. Removable storage unit 718, represents a floppy disk, magnetic tape, optical disk, etc. which is read by and written to by removable storage drive 714. As will be appreciated, the removable storage unit 718 includes a computer usable storage medium having stored therein computer software and/or data.

[0125] In alternative embodiments, secondary memory 710 may include other similar means for allowing computer programs or other instructions to be loaded into computer system 700. Such means may include, for example, a removable storage unit 722 and an interface 720. Examples of such may include a program cartridge and cartridge interface (such as that found in video game devices), a removable memory chip (such as an EPROM, or PROM) and associated socket, and other removable storage units 722 and interfaces 720 which allow software and data to be transferred from the removable storage unit 722 to computer system 700.

[0126] Computer system 700 may also include a communications interface 724. Communications interface 724 allows software and data to be transferred between computer system 700 and external devices. Examples of communications interface 724 may include a modem, a network interface (such as an Ethernet card), a communications port, a PCMCIA slot and card, etc. Software and data transferred via communications interface 724 are in the form of signals 728 which may be electronic, electromagnetic, optical or other signals capable of being received by communications interface 724. These signals 728 are provided to communications interface 724 via a communications path (i.e., channel) 726. This channel 726 carries signals 728 and may be implemented using wire or cable, fiber optics, a phone line, a cellular phone link, an RF link and other communications channels.

[0127] In this document, the terms "computer program medium" and "computer usable medium" are used to gen-

erally refer to media such as removable storage drive **714**, a hard disk installed in hard disk drive **712**, and signals **728**. These computer program products are means for providing software to computer system **700**. The invention is directed to such computer program products.

[**0128**] Computer programs (also called computer control logic) are stored in main memory **708** and/or secondary memory **710**. Computer programs may also be received via communications interface **724**. Such computer programs, when executed, enable the computer system **700** to perform the features of the present invention as discussed herein. In particular, the computer programs, when executed, enable the processor **408** to perform the features of the present invention. Accordingly, such computer programs represent controllers of the computer system **700**.

[**0129**] In an embodiment where the high-pressure flaking mill for creating the invention is implemented using software, the software may be stored in a computer program product and loaded into computer system **700** using removable storage drive **714**, hard drive **712** or communications interface **724**. The control logic (software), when executed by the processor **408**, causes the processor **408** to perform the functions of the invention as described herein.

[**0130**] In another embodiment, the high-pressure flaking mill for making the graphite nanostructures is implemented primarily in hardware using, for example, hardware components such as application specific integrated circuits (ASICs). Implementation of the hardware state machine so as to perform the functions described herein will be apparent to persons skilled in the relevant art(s). In yet another embodiment, the high-pressure flaking mill is implemented using a combination of both hardware and software.

[**0131**] As shown in **FIG. 4**, a second temperature sensor **132** and pressure sensor **134** are disposed on fluid jet **116** to measure the temperature and pressure of the fluid as it exits fluid jet **116** and enters first chamber **102**. The data from these sensors is also fed into signal conditioning module **402** and processor **408**.

[**0132**] A linear variable differential transducer (LVDT) **410** is disposed on one end of collider **128** of third chamber **128**. LVDT **410** measures the linear position of collider **128** with respect to the slurry flow as it enters third chamber **110**. The data from LVDT **410** are also fed into signal conditioning module **402** and processor **408**.

[**0133**] Finally, a particle size sensor **412** is disposed in outlet port **130** of third chamber **110** to measure the final size of the particles after mill processing is complete. The data from particle size sensor **412** are also fed into signal conditioning module **402** and processor **408**.

[**0134**] Although system **400** of **FIG. 4** is shown as only a data acquisition system, it would be apparent to one skilled in the relevant art, that processor **408** could use the data acquired to control mill processing of the graphite nanostructures. In such an embodiment, a feedback loop would be created between processor **408** and each of the chambers **102**, **104**, **106**, **108** and **110** to control the flow and flake processing at each stage of the processing.

[**0135**] For example, the user could select the final nanostructure size to be achieved via computer interface, and the data acquired by processor **408** could be used to vary the pressure of the fluid streams through the nozzles and/or to adjust the position of the flow restrictor with respect to the secondary slurry nozzle. In this way, the data acquired can

be used to control and accurately maintain the desired product size of the nanostructures.

[**0136**] The graphite can be recirculated into the high-pressure flaking mill **100** at any point throughout the processing. The characteristics of the nanostructures are somewhat pressure dependent. Typically, after a single pass through high-pressure flaking mill **100** the nanostructures have an average thickness of about 10 nm to 200 nm, and an aspect ratio of about 1,500:1 to 20,000:1, more commonly in the range of 1,500:1 to 8,000:1. Recirculation of the nanostructures at the same pressure results in further flaking along plane lines, resulting in smaller average thicknesses and higher aspect ratios. By contrast, recirculation of the nanostructures at a higher pressure results in breaking and cleaving of the platelets in a direction normal to the plane of the platelets, creating particles with smaller planar surface area.

[**0137**] Cleaving in directions normal to, or not along the plane of the platelet, exposes highly reactive catalytic surfaces along the breaks. These surfaces are useful for chemical reactions and purification, etc. Because untreated graphite reacts with passivating molecules or ions when cleaved, it is beneficial to treat and protect these highly reactive surfaces with protecting groups. One method of protecting these surfaces is to add a surfactant or a protecting group, such as a small chain organic material or a salt, to the fluid material of the high-pressure flaking mill. The surfactant or protecting group often takes a short time to fully protect the cleaved nanostructure. Accordingly, it is beneficial to introduce the surfactant or protecting group to the newly-exposed graphite at the earliest possible time, thereby reducing any oxidation that may occur prior to the time required to fully protect the surfaces. Nanostructures having protected catalytic surfaces exhibit better dispersion characteristics, more intimate mixing and faster and more complete reactions than graphite produced having unprotected surfaces.

[**0138**] Pressure in the high-pressure flaking mill also effects the efficiency of the flaking of graphite structures. For instance, at lower pressures, after a single pass, the nanostructures may be in the form of conglomerates of platelets, where each planar platelet is partially flaked from, but still attached to, the original graphite particle. In this case, recirculation of the graphite through the high-pressure flaking mill allows these conglomerates to be further broken down so that each original particle is fully divided or stripped into individual, isolated, independent platelets. In contrast, higher pressure during recirculation allows the graphite particles to be fully peeled into isolated, individual platelets with only a single pass.

[**0139**] Another advantage of the graphite nanostructures of the present invention is that the particles have very little surface charge compared to other particles, such as carbon black. This lack of surface charge is a result of the nearly instantaneous peeling or flaking that occurs when the graphite is processed in the high-pressure flaking mill. The very immediate and sudden pressure and release that is applied by the liquid jet of the high-pressure flaking mill causes peeling and flaking of graphite without prolonged rubbing or interaction that can develop surface charge. A low or nonexistent surface charge results in improved rheological characteristics when the particles are, in either a wet or a dry form, incorporated into slurries, composites and suspensions. Accordingly, nanostructures are easy to handle and evenly disperse as aggregate into a base compound.

[**0140**] Surface charge is measured by either a zeta-potential of the particles or by viscosity. When measured by

viscosity, a lower viscosity of a solution or suspension containing the particles corresponds to a lower surface charge of the particles. For example, a viscous polymer containing 50 wt % nanostructures has a lower viscosity than the same viscous polymer containing 50 wt % carbon black, or conventionally-milled graphite, or conventionally-expanded graphite. Lower surface charges allow for better dispersion of the particles. Accordingly, larger quantities of a material with a low surface charge can be blended into a material, with a consistent dispersion and better suspension.

[0141] The graphite nanostructures are manufactured by focusing kinetic energy of a high-pressure liquid to apply concentrated destructive forces on raw material feedstock, whether synthetic or natural. The high-pressure liquid causes extremely intensive turbulence, sharing, high-velocity collision, abrasion and destructive cavitation. These combined hydraulic forces cause the fluid to enter the tip of cracks, natural cleave planes, defects and high energy grain boundaries in the graphite, which creates tension at the tip. This tension causes hydro-wedging, in which the cracks propagate along the natural plane in the graphite, ultimately overcoming the Van der Waal forces and peeling the planar layers of the graphite so that small particles of the graphite separate into flakes or nanostructures. As such, the nanostructures of the present invention have a unique shape, viz, the smallest, thinnest natural platelet of the particle available. Particles generated using other methods which do not incorporate the high pressure techniques of the present invention do not result in flakes because they do not take advantage of the natural cracks in the graphite.

[0142] The high-pressure flaking mill can successfully flake other layered structures, such as coal, silicon dioxide, wollastonite, zirconia, alumina, ferrochrome, chromium metal, cordierite, boron nitride, natural and synthetic clays, polymers and others.

[0143] The graphite nanostructures resulting from processing using the high-pressure flaking mill can be utilized in a variety of applications. One example is to incorporate the nanostructures into a polymer or resin in specific amounts to customize properties of the resulting composite, such as stress, strain, impact strength and conductivity. Desired properties can be obtained or customized by varying filler content, matrix polymer type, and process techniques. Thermal, electrical, mechanical, chemical and abrasion properties are all affected by the form and matter of the particulate in polymers.

[0144] Polymer matrices containing graphite nanostructures show greater property enhancements than composites containing conventional graphite, carbon black and talc. The nanostructures of the present invention are characterized by a three-dimensional structure of highly-conductive platelets. Because of the platelet structure, the nanostructures provide significantly better three-dimensional connectivity and dispersion within the composite and matrix systems than particles of talc or conventional graphite. Furthermore, because of the thin, platelet structure, polymer/plastic resins can be filled with a higher percentage of the graphite nanostructures than with other materials which results in enhanced electrical, thermal and structural performance.

[0145] Nanostructure-filled polymer resins can be compounded utilizing conventional twin-screw extrusion techniques. The resulting extrudate can be compression molded, injection molded, extruded, cast, blow molded, vacuum formed, poltruded, and formed with other processes common to the plastics, pre-impregnated textiles, and polymeric

composites industries. Because of its platelet structure, introduction of nanostructures reduces molding pressures and shearing forces.

[0146] Appropriate thermosetting and thermoplastic polymers and materials for use with the nanostructures of the present invention include, but are not limited to, nylons, polyethylenes, polypropylenes, polystyrenes, polycarbonates, epoxies, polyimides, polyamides, fluorinated polymers, acryloides, polyacrylics, polyesters, cyanate esters and bismal imides.

[0147] Graphite, in general, can be used along with specially-processed electroconductive carbon black as a filler to provide electrical and thermal conductivity of normally non-conducting or poorly conducting polymeric materials. As earlier stated, graphite nanostructures have high specific surface area of about 10 m<sup>2</sup>/g to 20 m<sup>2</sup>/g, an average thickness of about 1 nm to 100 nm and a planar (platelet) morphology with an aspect ratio of at least 1,500:1. As described below, the morphological differences tend to make nanostructure-filled polymers more conductive and tend to give nanostructure-filled polymers greater thermal properties than carbon fiber filled composites.

[0148] Nanostructures may be incorporated into standard polymer extrusion methods, such as compression, injection, and blow molding; cast into films or sheets; vacuum formed as sheets; poltruded; or formed with other processes common to the plastics, pre-impregnated textiles, and polymeric composites industries.

#### Example

[0149] Composites of polypropylene and graphite nanostructures and nylon 6 and graphite nanostructures were tested in an effort to: (1) characterize tensile, flexural, impact, and thermal properties of samples molded from nanostructure-filled resins; (2) identify key property improvements offered by nanostructures and key property trends as a function of polymer type, filler type and size reduction technology; and (3) compare nanostructure-filled resins to those same resins in virgin, unmodified form as well as when filled with an identical weight percentage of conducting carbon black.

[0150] Both the polypropylene and the nylon 6 resins were standard injection molding grades. Nanostructures of 18  $\mu\text{m}$ (D<sub>50</sub>)/67  $\mu\text{m}$ (D<sub>100</sub>) particle size were introduced into both the polypropylene and the nylon 6 resins, resulting in "filled" resins. The filled resins were compounded in a twin-screw extrusion process in which both dry filler powders were fed into the molten resin to result in a 20% loading by weight and from which molding pellets were formed. The pellets were injection molded into mold tensile and flex bars, which were then subjected to standard ASTM tests for important mechanical properties, including flexural modulus, heat deflection temperature, tensile strength, electrical conductivity, and notched impact strength.

[0151] Polypropylene Resin

[0152] Table 1 shows the results of a study comparing the effects of graphite nanostructures introduced into polypropylene in varying quantities. As can be seen, the higher the weight percentage of graphite nanostructures, the greater the yield, tensile, and flexural values. As expected, the impact strength generally decreases with increased filler loading.

TABLE 1

Mechanical Properties of Nanostructure-Filled Polypropylene							
Polymer/ wt % Graphite Nano- structures	Yield Stress (PSI)	Tensile Modulus (PSI)	Flexural Modulus (PSI)	Elongation at Yield Point (%)	Elongation at Break Point (%)	Izod Impact Strength (ft*lb/in)	Heat Deflection Temp. (° C.)
Fina 7825	3563	47400	115000	5	715	0.76	46
5%	3920	56500	173700	4	592	0.68	48
10%	3896	59100	211000	4	490	0.67	49
20%	3916	63700	281000	6	71	0.69	55
36%	4100	85400	514000	3	13	0.40	65
53%	4516	94600	912000	5	6	0.40	82

[0153] Table 2 shows a comparison of properties for composites of polypropylene (PP) and either talc, CONDUCTEX carbon black or graphite nanostructures. As can be seen from the table, the composite containing graphite nanostructures had less stress and elongation at the yield point, less or equivalent loss of impact strength and a higher flexural modulus than either the talc or carbon black-filled composites.

TABLE 2

Comparison of Mechanical Properties of Polypropylene Composites				
Filler in PP	% Property Change at 20% Loading in PP			
	Stress at Yield Point	Elongation at Yield Point	Izod Impact Strength	Flexural Modulus
Talc	21%	-50%	-68%	130%
CONDUCTEX	31%	-45%	-49%	100%
Carbon Black				
Graphite	10%	-36%	-49%	199%
Nanostructure				

[0154] Nylon 6 Resin

[0155] Table 3 shows the results of a study comparing the effects of graphite nanostructures introduced into Nylon 6 in varying quantities.

[0156] The impact strength of the Nylon 6 and polypropylene composites was tested using a standard Izod test. In an Izod test, a pendulum swings on its track and strikes a notched, cantilevered plastic sample. The energy lost (required to break the sample) as the pendulum continues on its path is measured from the distance of its follow through. Addition of nanostructures to Nylon 6 resulted in significant increases in both the flexural and tensile moduli as well as the heat deflection temperature.

[0157] Table 4 shows measured values of mechanical and thermal characteristics of composite polymers filled with the commonly used carbon black and with graphite nanostructures, for direct comparison. As seen below, a polypropylene (designated by PP) composite having 20 wt % graphite nanostructures exhibited higher measured values for flexural modulus and heat deflection temperature than the same polymer with an equivalent weight of carbon black. Similar results were obtained using Nylon 6 as the polymeric matrix. The impact strength of all filled samples was reduced, though less than in the case of the filled polypropylene.

[0158] Measured values taken for a composite of polypropylene having 53 wt % graphite nanostructures are shown in Table 4. Composites of polypropylene having 53 wt % carbon black are not manufacturable due to the large increase in viscosity that occurs when carbon black is introduced into a polymer. While the nanostructures of the

TABLE 3

Mechanical Properties of Nanostructure-Filled Nylon 6							
Polymer wt % Graphite Nano- structures	Yield Stress (PSI)	Tensile Modulus (PSI)	Flexural Modulus (PSI)	Elongation at Yield Point (%)	Elongation at Break Point (%)	Izod Impact Strength (ft*lb/in)	Heat Deflection Temp. (° C.)
Capron	6650	260000	348000	6	32	1.13	58
8202							
10%	10350	421000	482000	**	5	0.80	70
20%	9460	499000	628000	**	5	0.68	82
40%	10440	1059000	1444000	**	4	0.62	173
50%	9890	1223000	1750000	**	3	0.52	205

Note: \*\* represents that the sample exhibited no evidence of a yield point prior to breaking, indicating a high degree of stiffening.

present invention can be loaded into polymers in weight-percentages exceeding 60%, carbon black must be loaded in significantly lower quantities.

lated form was manually dry mixed with graphite nanostructures at ambient temperature and then compression molded to generate test bars that were free of the shearing forces and

TABLE 4

Summary Of Changes In Properties: Unmodified Graphite Nanostructures ("GN") and Carbon Black as Fillers in Polypropylene and Nylon 6

Molded Composite	Filler Weight Loading	Tensile Modulus	Flexural Modulus	Stress at Yield Point	Elongation at Yield Point	Izod Impact Strength	Heat Deflection Temp.
PP/Carbon Black	20%	+21%	+100%	+31%	-45%	-49%	+13%
PP/GN	20%	+34%	+199%	+10%	-36%	-49%	+22%
PP/GN	53%	+100%	+693%	+27%	0%	-60%	+78%
Nylon 6/Carbon Black	20%	+35%	+11%	+29%	-43%	-16%	+21%
Nylon 6/GN	20%	+56%	+79%	**	**	-24%	+46%

Note: \*\* represents that the sample exhibited no evidence of a yield point prior to breaking, indicating a high degree of stiffening.

[0159] Conductivity

[0160] Conductivity tests were conducted to show the electrical properties of composites including the thin, planar structure of the graphite nanostructures. Conductivity measurements were taken of (1) nylon and polypropylene extruded molding pellets, (2) injection molded flex bars of nylon and polypropylene, and (3) graphite nanostructure/low density polyethylene resin compression molded bars.

[0161] A composite of nylon 6 having 20 wt % graphite nanostructures (about 10.5% graphite nanostructures by volume) improved electrical properties from insulating to conductive (10<sup>-8</sup> S/cm) in the extruded molded pellet form. In these initial tests, conductive properties were lost after injection molding, suggesting that the critical volume fraction (ϕ<sub>c</sub>) necessary for continuous conductivity was approached, but not exceeded.

[0162] With regard to polypropylene, a composite having 20 wt % graphite nanostructures by weight (about 9% by volume) was not sufficient to transition the composite from insulating to conducting in the extruded molded pellet form. However, field results at higher loading levels in polypropylene indicate conductivity at dissipative levels at 38 wt % loading, and full conductivity at 53 wt % loading. It is likely, therefore, that ϕ<sub>c</sub> for this size nanostructures in polypropylene falls in the 45 wt % (or 20-25 % by volume range).

[0163] At loadings as low as 10.5% by volume in nylon, the composite of nylon and graphite nanostructures showed signs of conductivity in a particle size range of 18 microns. Commercial graphite of average particle sizes of 26 and 51 microns did not show comparable levels of conductivity until loaded in low density polyethylene resin (LDPE) at 18% and 24% by volume, respectively. This suggests that the morphological structure of the graphite nanostructures provide a positive effect on the conductive nature of the graphite in a polymer matrix.

[0164] Because extrusion and injection molding affects the dispersion and alignment pattern of carbon particles in a polymer matrix, especially as observed in the polypropylene and Nylon 6 trials, experimentation to isolate from these effects was also undertaken. In these trials, LDPE in granu-

heat profiles common with extrusion and injection molding. Test bars of LDPE with 5% volume loading of graphite nanostructures were found to be somewhat conductive. Good conductivity was achieved at about 10% volume loading (about 20 wt %), and high conductivity (~3 log S/cm) at about 20% volume loading. This corresponds with commercial electroconductive carbon black in LDPE.

[0165] The morphology of the graphite nanostructures causes individual flakes to overlap in a host matrix material, leading to an increase in mechanical properties such as the modulus and thermal properties (heat deflection temperature). With respect to electrical conductivity, the overlapping graphite nanostructure flakes can result in higher conductivity values for a specific material. Polymeric matrices filled with graphite nanostructures are more conductive than other polymerics filled with other graphite materials currently being utilized.

[0166] As shown in Table 5 below, a 30 melt flow polypropylene copolymer with 3.5% ethylene having 20% graphite nanostructures shows an increase in the heat deflection temperature to equal that of a 22 melt flow nylon 6. Also, the flexural modulus of the nanostructure composite is increased such that it approaches the modulus of the unfilled nylon 6. The same polymer filled with 53% graphite nanostructures had a higher flexural modulus and a higher heat deflection temperature. Accordingly, properly selected composite materials of polypropylene-based graphite nanostructures (having higher molecular weight, homopolymeric) with properly-tailored quantities of graphite nanostructures may substitute for some engineering plastics such as nylon 6 in applications from which olefinic materials have been excluded due to the inherent ability of nylon to perform at higher temperatures. The incentive to switch to olefinic materials given comparable performance is economic, as polypropylene-based materials cost about 65% to 75% less than the cost of nylon 6.



TABLE 5

Comparison Of Key Properties Of Unfilled Nylon 6 and Nanostructure-Filled Polypropylene Copolymer					
Polymer/Filler	Yield Stress (PSI)	Yield Elongation (%)	Izod Impact Strength (ft.*lb./in.)	Flexural Modulus (PSI)	Heat Deflection Temperature (° C.)
Capron 8202 Nylon 6	8707	7	0.82	380,000	56
Fina 7825 PP + 20% Nanostructure	4370	7	0.55	305,000	56
Fina 7825 PP + 36% Nanostructure	4100	3	0.40	514,000	65

[0167] Finally, graphite nanostructures exhibit enhanced lubricating performance due to the Theological behavior of uniform flakes flowing freely past one another. The drag coefficient of spheres or expanded porous “worms” is far higher than well-dispersed, uniform, thin flakes of the present invention that produce classic laminar flow at the lowest viscosity possible.

[0168] While a number of embodiments of the present invention have been described above, it should be understood that they have been presented by way of example, and not limitation. It will be apparent to persons skilled in the relevant art that various changes in form and detail can be made therein without departing from the spirit and scope of the invention. Thus the present invention should not be limited by any of the above-described exemplary embodiments, but should be defined only in accordance with the following claims and their equivalents.

What is claimed is:

- 1. Graphite nanostructures in the form of platelets, wherein a majority of said platelets have an aspect ratio of at least 1,500:1.
- 2. The graphite nanostructures of claim 1, wherein a majority of said platelets have a footprint of about 10 μm×30 μm.
- 3. The graphite nanostructures of claim 1, wherein a majority of said platelets have a specific surface area of at least 5 m<sup>2</sup>/g.
- 4. The graphite nanostructures of claim 1, wherein a majority of said platelets have an average thickness of less than 100 nm.
- 5. Graphite nanostructures comprising a plurality of randomly-aligned platelets.
- 6. Graphite platelets, wherein a majority of the platelets have a specific surface area of at least about 5 m<sup>2</sup>/g and an average thickness of less than 100 nm.
- 7. The graphite platelets of claim 6, wherein said platelets are structurally independent and have a planar morphology and are of a geometrically angled shape.
- 8. The graphite platelets of claim 6, wherein the average thickness is less than 50 nm.
- 9. The graphite platelets of claim 6, wherein the average thickness is less than 20 nm.
- 10. The graphite platelets of claim 6, wherein the platelets have an average aspect ratio of at least 1,500:1.
- 11. The graphite platelets of claim 6, wherein the platelets have an average aspect ratio in the range of 1,500:1 to 20,000:1.

12. The graphite platelets of claim 6, wherein the platelets have an average aspect ratio in the range of 1,500:1 to 8,000:1.

13. The graphite platelets of claim 6, wherein a majority of the platelets have an angular periphery.

14. Graphite platelets, wherein a majority of the platelets have an aspect ratio of at least 1,500:1, and an individual, average flake thickness of less than 100 nm.

15. The graphite platelets of claim 14, wherein a majority of the platelets are structurally independent and have a planar morphology.

16. The graphite platelets of claim 14, wherein a majority of the platelets have an angular periphery.

17. The graphite platelets of claim 14, wherein the average thickness is less than 50 nm.

18. The graphite platelets of claim 14, wherein the average thickness is less than 20 nm.

19. The graphite platelets of claim 14, wherein the average aspect ratio is in the range of 1,500:1 to 100,000.

20. The graphite platelets of claim 14, wherein the average aspect ratio is in the range of 1,500:1 to 20,000:1.

21. The graphite platelets of claim 14, wherein the average aspect ratio is in the range of 1,500 to 8,000:1.

22. A method for fracturing graphite particles into platelets, comprising:

introducing the graphite into a high-pressure flaking mill, wherein said high-pressure flaking mill causes a hydro-wedging effect that overcomes the Van der Waal forces of the particles and fractures said particles into platelets.

23. The method of claim 22, wherein a majority of the platelets have an aspect ratio of at least 1,500:1.

24. A polymer matrix composite, comprising:

a polymer; and

graphite platelets having a specific surface area of at least about 5 m<sup>2</sup>/g and an individual, average platelet thickness of less than 100 nm.

25. The polymer matrix composite of claim 24, wherein said polymer is selected from the group consisting of: nylons, polyethylenes, polypropylenes, polystyrenes, polycarbonates, epoxies, polyimides, polyamides, fluorinated polymers, acryloides, polyacrylics, polyesters, cyanate esters and bismal imides.

\* \* \* \* \*